

## **Copyright Warning & Restrictions**

The copyright law of the United States (Title 17, United States Code) governs the making of photocopies or other reproductions of copyrighted material.

Under certain conditions specified in the law, libraries and archives are authorized to furnish a photocopy or other reproduction. One of these specified conditions is that the photocopy or reproduction is not to be “used for any purpose other than private study, scholarship, or research.” If a user makes a request for, or later uses, a photocopy or reproduction for purposes in excess of “fair use” that user may be liable for copyright infringement,

This institution reserves the right to refuse to accept a copying order if, in its judgment, fulfillment of the order would involve violation of copyright law.

**Please Note: The author retains the copyright while the New Jersey Institute of Technology reserves the right to distribute this thesis or dissertation**

Printing note: If you do not wish to print this page, then select “Pages from: first page # to: last page #” on the print dialog screen

The Van Houten library has removed some of the personal information and all signatures from the approval page and biographical sketches of theses and dissertations in order to protect the identity of NJIT graduates and faculty.

## ABSTRACT

### PREDICTION OF LINEAR AND NON-LINEAR COMPONENTS OF CUTTER DEFLECTION IN END MILLING TOOLS

by  
Kimberly C. Nazimek

In this study, cutter length, cutter diameter, depth of cut, and magnitude of the instantaneous force vector are examined to determine their effects on cutter deflection during end milling. Their contributions to both linear and non-linear cutter deflection are examined. Models are developed to compute deflection for both flat and ball end mills. These models are evaluated to determine the contribution of each type of deflection encountered during a variety of milling conditions. A discussion on the transfer of deflection data to an estimation of machining accuracy is then presented.

PREDICTION OF LINEAR AND NON-LINEAR COMPONENTS OF CUTTER  
DEFLECTION IN END MILLING TOOLS

by  
Kimberly Nazimek

A Thesis  
Submitted to the Faculty of  
New Jersey Institute of Technology  
in Partial Fulfillment of the Requirements for the Degree of  
Masters of Science in Manufacturing Systems Engineering

Manufacturing Engineering Division

January 1994

APPROVAL PAGE

PREDICTION OF LINEAR AND NON-LINEAR COMPONENTS OF CUTTER  
DEFLECTION IN END MILLING TOOLS

Kimberly C. Nazimek

Dec. 21, 1993

Dr. Ming Leu, Thesis Advisor  
Professor of Mechanical Engineering, NJIT

Date

Dr. Denis Blackmore, Committee Member  
Professor of Mathematics, NJIT

1/3/94

Date

Dr. Raj Sodhi, Committee Member  
Director of Manufacturing Engineering Program, NJIT

1/3/94

Date

Blank Page

## BIOGRAPHICAL SKETCH

**Author:** Kimberly C. Nazimek

**Degree:** Master of Science in  
Manufacturing Systems Engineering

**Date:** January 1994

**Date of Birth:**

**Place of Birth:**

### Undergraduate and Graduate Education:

- Masters of Science in Manufacturing Systems Engineering, New Jersey Institute of Technology, Newark, NJ, 1994
- Masters of Science in Aerospace Engineering, West Virginia University, Morgantown, WV, 1989
- Bachelor of Science in Aerospace Engineering, West Virginia University, Morgantown, WV, 1987

**Major:** Manufacturing Systems Engineering

### Presentations and Publications:

Cronin, K. and M. Lyell "Study of Velocity Gradient Effects on Extinction Properties of Premixed Laminar Flames in Normal and Oblique Stagnation Flows via a Finite Element Formulation." *AIAA 27th Aerospace Sciences Meeting*. Reno, Nevada, 9-12 January 1989.

## ACKNOWLEDGEMENT

The author would like to thank her research advisor Dr. Ming Leu for the support and advice given during her studies at New Jersey Institute of Technology. She would also like to express her appreciation to Dr. Denis Blackmore and Dr. Raj Sodhi for serving on her advisory committee.



## TABLE OF CONTENTS

Chapter	Page
1 INTRODUCTION.....	1
1.1 Motivation.....	1
1.1.1 Background.....	1
1.1.2 Relevant Studies.....	2
1.2 Objective.....	5
2 CUTTING FORCE CALCULATION.....	6
2.1 Force Model Requirements.....	6
2.2 Cutting Force Model Definition.....	7
2.2.1 Flat End Mills.....	7
2.2.2 Ball End Mills.....	10
3 DEFLECTION MODEL FORMULATION.....	12
3.1 Deflection Model Requirements.....	12
3.2 Deflection Model Definition.....	12
3.2.1 Linear Deflection.....	12
3.2.2 Non-Linear Deflection.....	14
3.3 Deflection of Ball End Mills.....	17
3.3.1 Linear Deflection of Ball End Mills.....	17
3.3.2 Non-Linear Deflection of Ball End Mills.....	18
4 EVALUATION OF LINEAR AND NON-LINEAR END MILL DEFLECTION COMPONENTS.....	20
4.1 Analysis Methodology.....	20
4.2 Force Model Output.....	20
4.3 Evaluation of Deflection Components.....	23
4.3.1 Variation with Force.....	23
4.3.2 Variation with Cutting Depth.....	27

TABLE OF CONTENTS  
(Continued)

Chapter	Page
4.4 Transferring Deflection Results Into a Machining Error Determination.....	31
5 CONCLUSION.....	32
5.1 Conclusions.....	32
5.2 Suggestions for Future Work.....	32
REFERENCES.....	33

## LIST OF TABLES

Table	Page
3.1 End mill deflection determined through CAE analysis and its comparison with experimental results.....	15

## LIST OF FIGURES

Figure	Page
2.1 Cutting force model .....	facing 7
2.2 Cutting force model illustration for ball end mills.....	facing 10
3.1 Linear tool deflection model.....	facing 13
3.2 Example I-DEAS finite element model used to represent a flat end mill.....	facing 18
3.3 Example I-DEAS finite element model used to represent a ball end mill.....	facing 18
3.4 Comparison of flat end mill to ball end mill deflection results under equal loading.....	19
4.1 Sample force model output.....	21
4.2 Non-linear end mill deflection for various cutting forces $D=12.7$ mm.....	facing 24
4.3 Linear end mill deflection for various cutting forces $D=12.7$ mm.....	facing 24
4.4 Combined end mill deflection for various cutting forces $D=12.7$ mm.....	24
4.5 Non-linear end mill deflection for various cutting forces $D=18.14$ mm.....	facing 25
4.6 Linear end mill deflection for various cutting forces $D=18.14$ mm.....	facing 25
4.7 Combined end mill deflection for various cutting forces $D=18.14$ mm.....	25
4.8 Non-linear end mill deflection for various cutting forces $D=20.0$ mm.....	facing 26
4.9 Linear end mill deflection for various cutting forces $D=20.0$ mm.....	facing 26
4.10 Combined end mill deflection for various cutting forces $D=20.0$ mm.....	26

LIST OF FIGURES  
(Continued)

Figure	Page
4.11 Non-linear end mill deflection for various cutting depths with constant force loading D=12.7 mm.....	facing 28
4.12 Linear end mill deflection for various cutting depths with constant force loading D=12.7 mm...	facing 28
4.13 Combined end mill deflection for various cutting depths with constant force loading D=12.7 mm.....	28
4.14 Non-linear end mill deflection for various cutting depths with constant force loading D=18.14 mm.....	facing 29
4.15 Linear end mill deflection for various cutting depths with constant force loading D=18.14 mm..	facing 29
4.16 Combined end mill deflection for various cutting depths with constant force loading D=18.14 mm.....	29
4.17 Non-linear end mill deflection for various cutting depths with constant force loading D=20.0 mm.....	facing 30
4.18 Linear end mill deflection for various cutting depths with constant force loading D=20.0 mm...	facing 30
4.19 Combined end mill deflection for various cutting depths with constant force loading D=20.0 mm.....	30

## CHAPTER 1

### INTRODUCTION

In the introduction, the motivation and objectives of this study will be defined. This is achieved by examining existing literature and ongoing studies in the relevant areas. Through a discussion of the related background research and ongoing studies, the motivation for the current study will become apparent. The objectives of the study are then defined.

#### 1.1 Motivation

##### 1.1.1 Background

Commercial CAD/CAM software packages, such as ProEngineer or I-DEAS, are becoming increasingly popular for use in the mechanical design and manufacture of parts. These software promote concurrent engineering techniques and enable quick changes to part design and generation of resultant tool path planning programs needed to operate NC machining equipment. Present tool path planning programs inside these software, however, neglect consideration of the machining process physics even though several predictive models have been developed [Altintas & Spence, 91]. These CAD/CAM programs rely on the experience of the user to select a reasonable spindle speed, cutting depth, cutting width, etcetera, which when used to calculate a tool path for manufacture of the part, will not

result in large machining errors due to deflections of the cutting tool.

Cutter deflection in end milling is a topic currently under investigation in a number of studies for a variety of reasons. The motivation for one such study is the fact that although deflection adversely affects the accuracy of milling operations, flexibility of the cutter is beneficial in attenuating chatter and overload in sudden transient situations [Bertok,83]. Although machining error is caused by many factors, tool deflection has been determined to be the single most significant factor in end milling operations, particularly when slender milling tools are being utilized [Kline, DeVor, & Shareef,82]. Therefore, in end milling operations, deflection of the cutter is an important factor affecting the accuracy of machining, and has implications on the selection of cutting parameters.

#### **1.1.2 Relevant Studies**

In an ongoing study at the University of Tokyo, a cutting simulation for machinability evaluation using an extended Z buffer model representing a workpiece and tool swept volume is being developed [Takata & Tsai,89]. This simulation predicts the instantaneous cutting force vectors acting on a square end mill. The tool deflection induced by the cutting force is then calculated and the results are used to estimate the machining error caused by tool deflection. The deflection model in this simulation assumes the interfaces between the

tool, chuck, and collet are the weakest part and the displacements at these parts account for most of the tool deflection. The tool deflection in this simulation, therefore, is assumed to be linear. Actual tool deformation and its contribution to tool deflection is ignored.

In a related study [Kops & Vo,90], end mill deflection due to the deformation of the end mill was determined through CAE analysis and compared to experimental results. Deflection was calculated under static load conditions representing a range of typical cutting conditions. Experimental results were obtained using strain gauges mounted on the end mill. This permitted the separation of the cutter deformation from the deflection of the spindle assembly and the displacement of the tool in the collet. Results of this study demonstrated that under various loading conditions the deflection of the tool due to tool deformation can be significant. An equivalent diameter,  $D_e$ , solid cylinder yielding the same deflection under identical loading conditions as the cutter, and having, therefore, the same moment of inertia,  $I$ , as the cutter is identified through CAE analysis. End mill deflection due to cutter deformation can then be estimated using cantilever beam theory subject to intermediate loading with  $I = \pi * D_e^4 / 64$ .

In another study on the prediction of surface accuracy in end milling [Kline, DeVor, Shareef,82], deflection of the end mill was estimated by modeling the cutter as a cantilever beam, rigidly supported by the tool end holder. The end mill



deflects due to cutting forces applied as point forces at force centers. Cutter deflections due to interfaces between the tool, chuck, and collet are taken into account by using an effective length,  $L$ , slightly larger than the actual cutter, which gave results closer to experimental results. The moment of inertia of the end mill in this simulation was assumed to be  $I = D^4/48$ .

Each of the deflection models in the above studies provided effective results for the milling conditions under consideration in the studies. None of the studies, however, provide a detailed analysis of the separate contributions of the linear deflection due to interfaces between the tool, chuck, and collet, and the non-linear deflection due to tool deformation. It is certain that under some milling conditions tool deformation has very little effect on the deflection of the cutter. Under other milling conditions, tool deformation can not be ignored. This study will attempt to clarify the contributions of the linear and non-linear modes of deflection for a variety of cutting conditions.

All of the deflection models examined to date deal strictly with flat end mills. No attempt has been made to develop a model for ball end mills which are commonly used for finishing cuts in end milling. This study will attempt to eliminate this shortcoming.

## 1.2 Objective

In this study, cutter length, cutter diameter, depth of cut, and magnitude of the instantaneous force vector are examined to determine their effects on cutter deflection during end milling. Their contributions to both linear and non-linear cutter deflection are examined. Linear and non-linear end mill deflection models are developed based on recent studies in this area of interest.

Geometrical and technological information about the workpiece and machine tool data are used as inputs to two FORTRAN sub-programs which compute the cutting force estimation, and tool deflection estimation. Models are developed for both the flat and ball end mills. These models are evaluated to determine the contribution of each type of deflection encountered during a variety of milling conditions. Finally, a discussion on the transfer of the deflection data to an estimation of machining accuracy is presented.

## CHAPTER 2

### CUTTING FORCE PREDICTION

#### 2.1 Force Model Requirements

The cutting force is one of the most important process parameters in a cutting operation. The cutting force is related to a number of abnormal occurrences such as tool breakage, excessive tool wear, chatter vibration, and tool deflection.

In the physical simulation of cutter deflection during milling, the force vector at a certain instance must first be calculated using a force model. Most cutting simulations have used the model based on the empirical equation representing the cutting force as proportional to the volume of removed metal [Wang,87] [Bertok,83]. This method, however, can estimate only the average cutting force and does not provide the instantaneous force vector which is necessary for accurate estimation of the tool deflection. It is therefore necessary to adopt a force model where the tool is divided into small sections along the axis of the tool and calculate the force vector acting on each section [Kline,82].

In section 2.2, the cutting force model used in this study is defined first for flat end mills, then extended for use with ball end cutters. The flat end mill force model is based on work completed by previous researchers. The formulation of an extension to ball end mills is original.

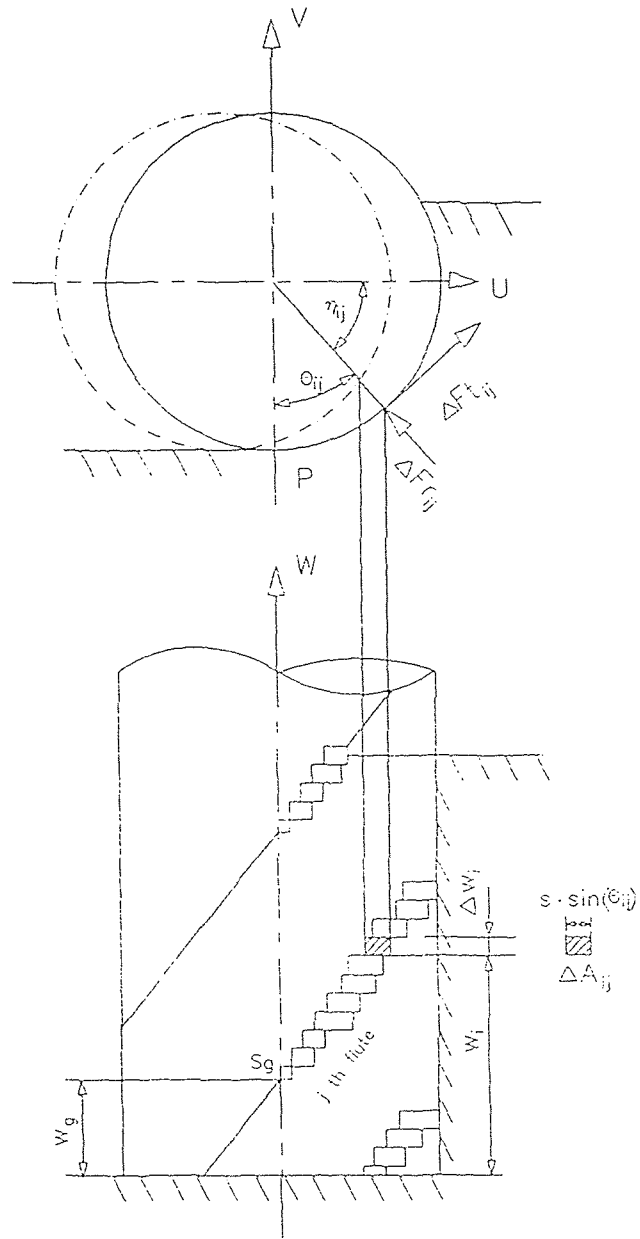


Figure 2.1 Cutting force model.

## 2.2 Cutting Force Model Definition

### 2.2.1 Flat End Mills

In the physical simulation of the cutter deflection during milling, the force vector at a certain instance is first calculated using a force model. To meet our needs, it was necessary to adopt a model where the tool is divided into small sections along the axis of the tool and calculate the force vector acting on each section in contact with the workpiece. These force vectors are then summed over the sections in contact with the workpiece, and the instantaneous cutting forces are obtained. The force model used by Tsai & Takata for flat end milling tools [Tsai & Takata,90] was adopted. Figure 2.1 illustrates this cutting force model.

In the model illustration, the u-axis represents the feed direction, while the v-axis represents the direction perpendicular to the u-axis. The instantaneous cutting forces for flat end mills can be computed by summing the force vectors acting on the flutes of each divided section in contact with the work piece. In this manner, the force in the cutting direction,  $F_u$ , and the force perpendicular to the cutting direction,  $F_v$ , for flat end mills can be calculated using the formulas which follow, where, the subscripts  $i$  and  $j$  denote that the variables are related to the  $j$ -th flute of the  $i$ -th divided section called the  $i,j$ , cutting edge.  $\eta_{i,j}$  is the angle between the  $i,j$  cutting edge and the u axis.  $\Delta Fr_{i,j}$  and  $\Delta Ft_{i,j}$  are the radial and tangential forces acting on the  $i,j$  cutting edge.

$$F_u = \Sigma(\Delta F_{t_{i,j}} \sin(\eta_{i,j}) - \Delta F_{r_{i,j}} \cos(\eta_{i,j})) \quad (2.1)$$

$$F_v = \Sigma(\Delta F_{t_{i,j}} \cos(\eta_{i,j}) + \Delta F_{r_{i,j}} \sin(\eta_{i,j}))$$

The above forces are proportional to the chip element removed by the  $i,j$  cutting edge,  $\Delta A_{i,j}$ , as denoted in the equations below.

$$\Delta F_{t_{i,j}} = K_t \Delta A_{i,j} \quad (2.2)$$

$$\Delta F_{r_{i,j}} = K_r \Delta A_{i,j}$$

The chip element removed by the  $i,j$  cutting edge is calculated using the following equation where  $s$  is the feed per tooth,  $\Delta W_i$  is the thickness of the  $i$ -th tooth section and  $\theta_{i,j}$  is the angular cutting position of the  $j$ -th flute of the  $i$ -th divided section relative to the  $v$ -axis.

$$\Delta A_{i,j} = s \sin(\theta_{i,j}) \Delta W_i \quad (2.3)$$

The constants  $K_t$  and  $K_r$ , in (2.2), are estimated from experimental data as outlined in previous research [Takata & Tsai, 89]. These constants are machine dependent and will vary from one machining center to another. To determine  $K_t$  and  $K_r$ , Takata and Tsai conducted a series of tests using a throw away type, one-flute, straight tooth end mill cutter. During

cutting operations, the cutting force was measured by a 3-axis tool dynamometer installed between the workpiece and the table. A number of peripheral and end millings were executed under various cutting conditions and the tangential and radial cutting forces were calculated from the measured cutting force in the u and v directions. The constants  $K_t$  and  $K_r$  are not, however, independent of cutting conditions. To determine their values for various cutting conditions, Takata and Tsai constructed the equations below, where  $K_{ct}$  and  $K_{cr}$  are constants determined by the material of the workpiece,  $K_p$  is a correction factor which increases in value from 1.0 to 1.2 during the initial spindle rotation of 2/100 degree immediately after the entrance of the flute into the cut,  $K_s$  is a correction factor for the feed rate (S), and  $K_{vt}$  and  $K_{vr}$  are correction factors for the cutting speed.

$$K_t = K_{ct} K_p (K_s/S)^{0.5} (1 - K_{vt} V) \quad (2.4)$$

$$K_r = K_{cr} K_p (K_s/S)^{0.5} (1 - K_{vr} V)$$

To obtain an accurate prediction of the forces encountered during milling, it is thus necessary to carry out the type of experiment described above for each machining center of interest. Once the constants are obtained, the force encounter during milling for a large number of milling conditions can be simulated with relative ease. These

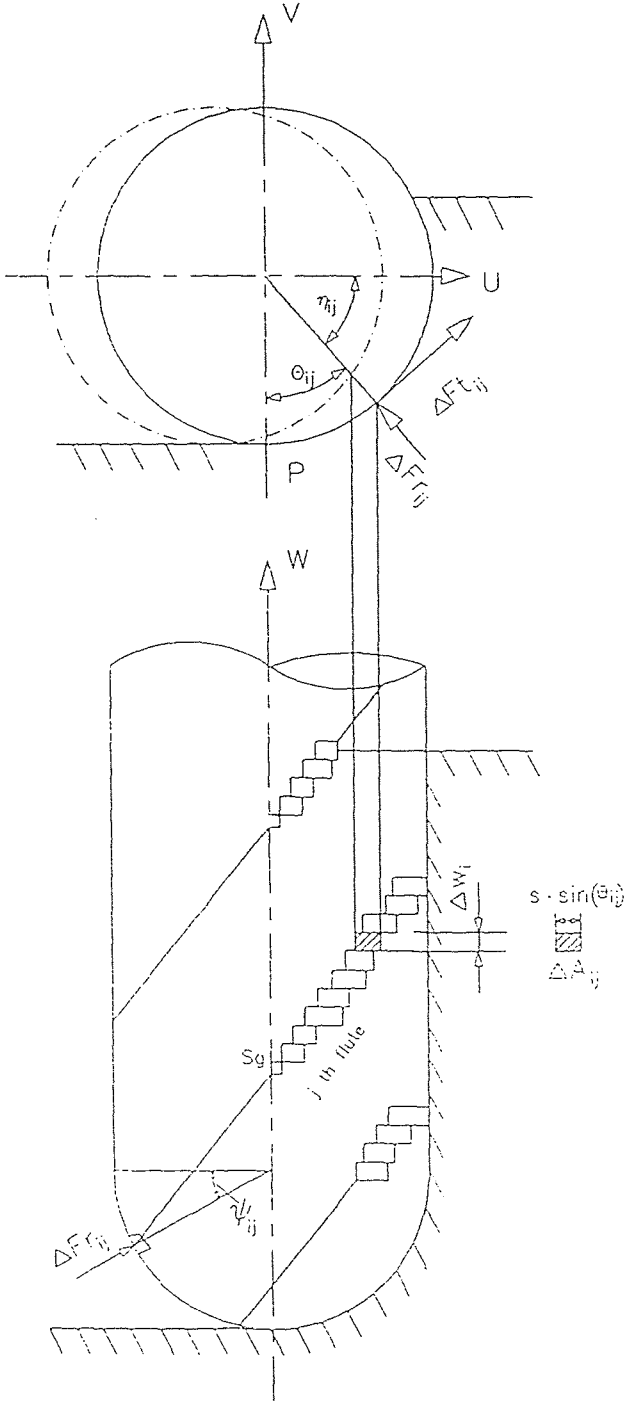


Figure 2.2 Cutting force model illustration for ball end mills.



instantaneous forces can then be used to estimate the deflection in the tool.

Cutting experiments were not conducted to support this study. A variety of literature exists on the estimation of these constants for different machining centers [Armarego & Deshpande,89], [Armarego & Deshpande,91], [Whitfield,88]. The literature was reviewed and machine constants were selected from the previous research experiments conducted in this field to meet our needs.

### 2.2.2 Extension to Ball End Mills

The above cutting force algorithms can be extended to ball end mills with a slight modification. Figure 2.2 illustrates this extension.

In the model for ball end mills, as in the model for flat end mills, the u-axis represents the feed direction, while the v-axis represents the direction perpendicular to the u-axis. The instantaneous cutting forces are computed by summing the force vectors acting on the flutes of each divided section in contact with the work piece. The cutting forces for ball end mills can thus be computed using the equations which follow,

$$F_u = \Sigma(\Delta F_{t_{i,j}} \sin(\eta_{i,j}) - \Delta F_{r_{i,j}} \cos(\psi_{i,j}) \cos(\eta_{i,j})) \quad (2.5)$$

$$F_v = \Sigma(\Delta F_{t_{i,j}} \cos(\eta_{i,j}) + \Delta F_{r_{i,j}} \cos(\psi_{i,j}) \sin(\eta_{i,j}))$$

where,  $\psi_{i,j}$  is the angle between the  $i,j$  cutting edge and the  $u,v$  plane as depicted in Figure 2.2.

## CHAPTER 3

### DEFLECTION MODEL FORMULATION

#### 3.1 Deflection Model Requirements

Tool deflection encountered during end milling can be characterized into two types of cutter deflection. One is a linear deflection due to interfaces between the cutting tool, the chuck, and the collet. The second is a non-linear deflection due to tool deformation. Any complete study of tool deflection encountered during end milling must take into consideration both types of deflection.

The deflection model chosen for use in this study is a combination of a linear deflection model developed at the University of Tokyo and a non-linear model formulated as an extension of a study on non-linear tool deformation conducted at the McGill University.

#### 3.2 Deflection Model Definition

##### 3.2.1 Linear Deflection

The simulation developed at the University of Tokyo [Takata & Tsai,89] uses a deflection model which assumes the interfaces between the tool, chuck and collet are the weakest part and the displacements at these parts contribute to most of the tool deflection. In this simulation, the tool deflection is represented by the linear displacement of the

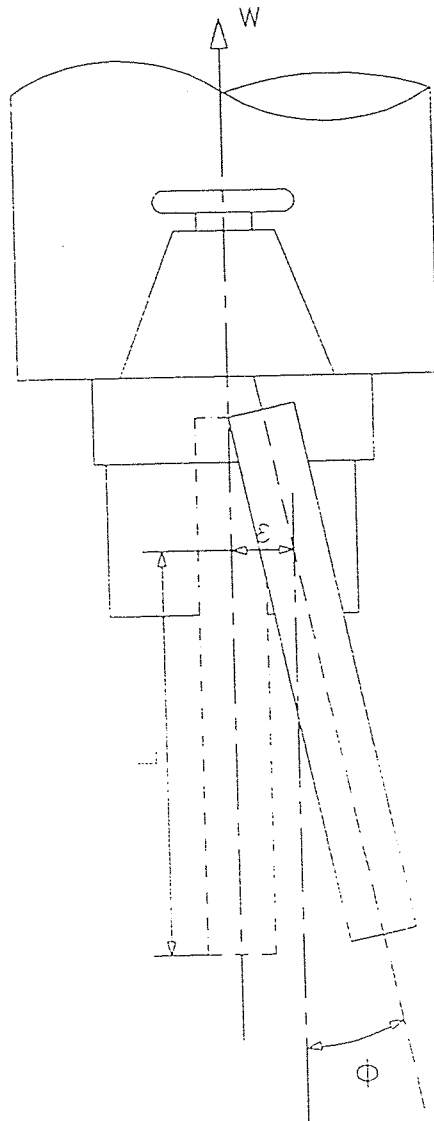


Figure 3.1 Linear tool deflection model.

tool measured at the center of the chuck,  $\epsilon$ , and the angular displacement of the tool,  $\phi$ , as depicted in Figure 3.1.

The linear deflection of the end mill due to interfaces between the tool, chuck and collet in the u ( $\delta_u$ ) and v ( $\delta_v$ ) directions based on this type of model are given by

$$\delta_v(W_i) = E_h Fv + E_r Mu (L - W_i) \quad (3.1)$$

$$\delta_u(W_i) = E_h Fu + E_r Mv (L - W_i)$$

where,  $E_h$  and  $E_r$  are constants determined by the structure of the machine, chuck, and collet. These constants were obtained by applying a static load to the tool mounted in the chuck and measuring the deflection at several points along center of the tool axis. Linear and angular displacements were obtained by plotting this data.  $Mu$  and  $Mv$  are moments generated by the forces in the u and v directions around the point corresponding to the center of the chuck and can be calculated using the equations below.

$$Mv = \Sigma[\Delta Fu_{i,j} * (L - W_i)] \quad (3.2)$$

$$Mu = \Sigma[\Delta Fv_{i,j} * (L - W_i)]$$

It is important to note that the machined surface is generated by the flute of the tool section whose angular

position,  $\theta_{ij}$ , is zero. As the tool rotates, the position of surface generation,  $S_g$ , moves upward and the machined surface corresponding to point P in Figure 2.1 is generated. Therefore, the machining error at each position along the w-axis, resulting from a deflection of the tool, can be estimated from the tool deflection in the v direction for this type of cut.

### 3.2.2 Non-Linear Deflection

Beginning with a study conducted at the McGill University [Kops & Vo,90], a model was formulated to calculate the non-linear deflection of the end mill due to tool deformation encountered during the milling process. Deflection of the end mill in the Kops & Vo study was determined through CAE analysis and compared to experimental results. Deflections were measured experimentally under static load conditions representing a range of typical cutting conditions. Results were obtained using strain gauges mounted on the end mill to permit the separation of the cutter deflection from the deflection of the spindle assembly and the displacement of the tool in the collet. CAE results were obtained using an I-DEAS generated finite element linear static analysis. Boundary conditions consisting of restraints and loads were specified. The end mill was treated as a cantilever beam acted upon by an intermediate concentrated load. Results of the study, reproduced here, in part, in Table 3.1, demonstrate that under various loading conditions, the deflection of the tool due to

tool deformation can be significant. The CAE results obtained using the I-DEAS generated finite element model of the milling tool gave results accurate to within 7.3%.

**Table 3.1** End mill deflection determined through CAE analysis and its comparison with experimental results.

End Mill Data		Loading Condition		Maximum Deflection		
D (mm)	$N_f$	F (N)	a (mm)	$\delta_m, CAE$ ( $\mu m$ )	$\delta_m, EXP$ ( $\mu m$ )	Diff. %
12.70	2	596	9.525	81.1	86.2	6.3
		160	6.350	27.9	26.0	6.8
		449	6.350	71.6	73.3	2.4
18.14	4	1000	14.290	26.9	25.7	4.5
		516	14.290	14.2	13.8	2.3
		703	9.525	24.8	26.6	7.3
		343	4.765	14.8	15.8	6.8

In Table 3.1, D is the diameter of the end mill,  $N_f$  is the number of flutes, F is the loading force, and a is the point of force application measured from the bottom of the end mill. The 12.70 mm end mill had a length of 40.74 mm while the 18.14 mm end mill had a length of 41.78 mm.

A study was then conducted using I-DEAS finite element analyzer (FEA) to determine an equivalent diameter, ( $D_c$ ), solid cylinder that when subjected to equal loading conditions as an end mill of equal length, would yield the same deflection results. The study found that a solid cylinder with approximately 0.8 times the diameter of a cutter would

give the same deflection results as a cutter under equal loading conditions within 7%. Results suggest that  $D_e$  could be generalized to 80% of the cutter diameter. More accurate results are obtained, however, if a CAE analysis is conducted to determine the exact  $D_e$ .

With this information in mind, a non-linear deflection model that gives fast and relatively accurate estimates of the non-linear deflection of the cutter using the empirical equations for deflection of cantilever beams with uniform cross sections with intermediate loads can be developed.

Since  $F_v$  and  $F_u$  have been computed using (2.1) and  $M_v$  and  $M_u$  have been computed using (3.2), it is possible to determine the placement of the resultant forces at single point locations ( $a_v$ ,  $a_u$ ) which will give the same beam deflection as the distributed cutting force with the equations below.

$$a_v = M_v/F_v$$

$$a_u = M_u/F_u$$
(3.3)

The deflection of the tool in the  $u$  and  $v$  directions at any point along the tool's length,  $W_i$ , can then be calculated. The deflection between the collet and the load ( $\delta_{AB_k}$ ) and between the load and the end of the mill ( $\delta_{BC_k}$ ), where the subscript  $k = u, v$  in turn, are given by the equations which follow, where  $L$  is the length of the tool from the center of the collet to the tip,  $E$  is the modulus of elasticity of the



tool material, and  $I$  is the moment of inertia of the equivalent diameter cylinder given by  $I = \pi * D_e^4 / 64$ .

$$\delta_{AB_k}(W_i) = F_k(L - W_i)^2 / 6EI [(L - W_i) - 3a_k] \quad (3.4)$$

$$\delta_{BC_k}(W_i) = F_k(a_k)^2 / 6EI [a_k - 3(L - W_i)]$$

The total deflections in the  $u$  and  $v$  directions resulting from the combination of the linear and non-linear portions of the tool deflection can then be estimated by adding the results of equations 3.1 and 3.4.

### 3.3 Deflection of Ball End Mills

The deflection model formulations defined in section 3.2 were developed for flat end mills. A major objective of this study, however, is to develop a deflection model compatible with ball end mills which are commonly used to perform finishing cuts. Sections 3.3.1 and 3.3.2 discuss the applicability of the previous deflection model formulation to ball end mills.

#### 3.3.1 Linear Deflection of Ball End Mills

The linear deflection model for flat end mills can be used as is for ball end mills. The deflection constants were obtained by applying a static load to the tool mounted in the chuck, measuring the deflection at several points along center of the tool axis, and plotting the data to determine the deflection.

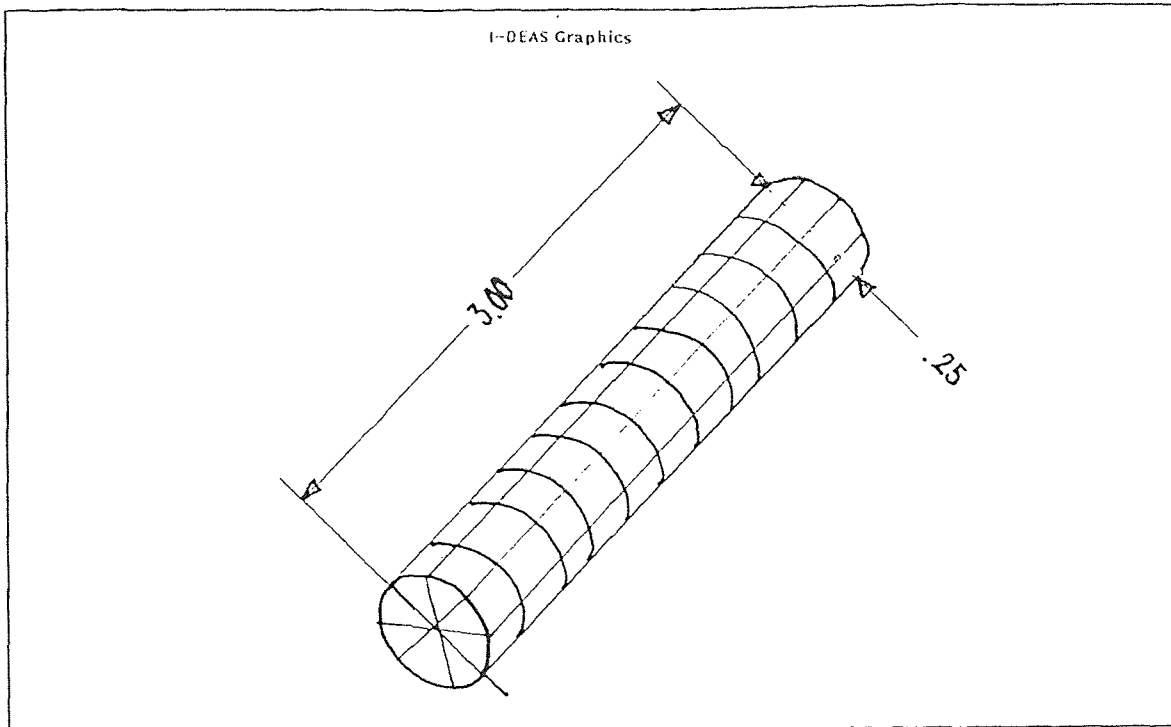


Figure 3.2 Example I-DEAS finite element model used to represent a flat end mill.

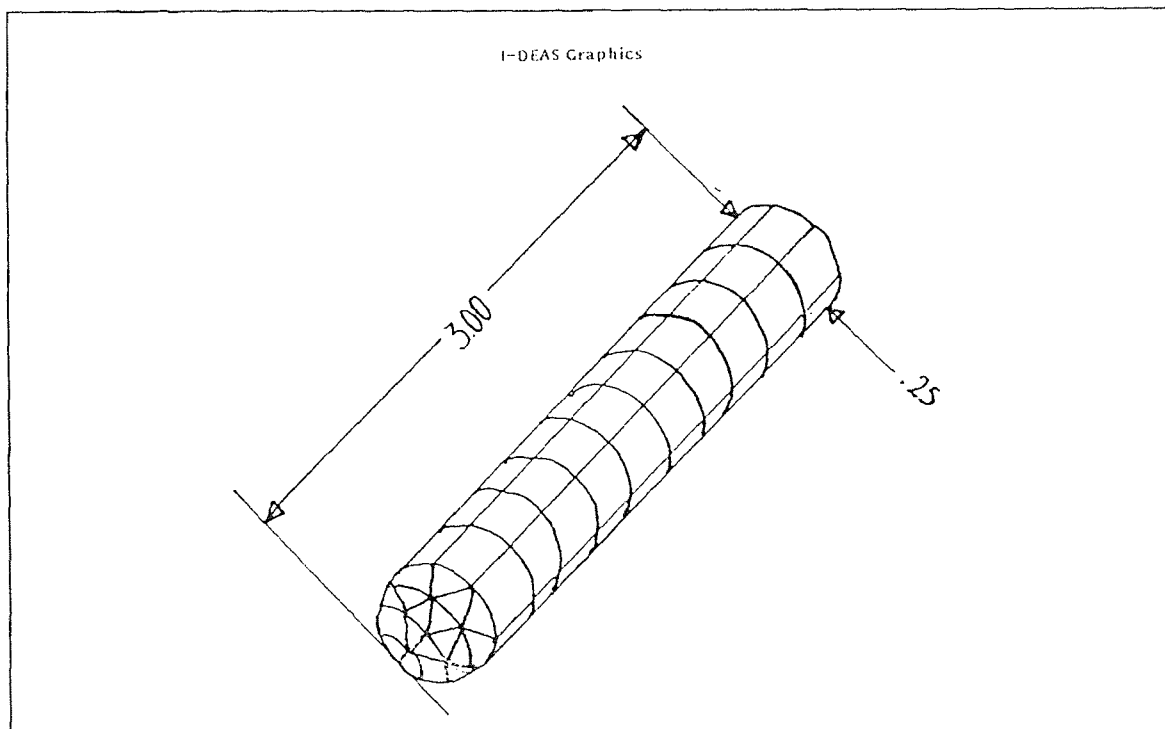


Figure 3.3 Example I-DEAS finite element model used to represent a ball end mill.

Deflection constants can be obtained for ball end mills in the same manner.

### 3.3.2 Non-linear Deflection of Ball End Mills

The calculation of non-linear deflection due to tool deformation for flat end mills is based on the fact that the tool has a uniform cross sectional area all along its length. For ball end mills, this does not hold true. To utilize the non-linear deflection model, it was assumed that the change in cross sectional area experienced at the tip of the cutter would have very little effect on the deflection results.

To verify this assumption, a finite element analysis comparison of flat end to ball end cutters of equal diameter and equal length with equal loading was conducted using the CAD/CAM solid modeling software I-DEAS.

The Kops and Vo study demonstrated that modeling an end mill as a solid cylinder with an equivalent diameter of 0.8 times the diameter of the cutter will give equivalent results. With this in mind, the finite element analysis was conducted on a solid cylinder and a solid cylinder with a rounded ball tip. Figures 3.2 and 3.3 depict one set of the finite element models used in this study. Boundary conditions consisting of restraints and loads were specified. The end mill was treated as a cantilever beam acted upon by an intermediate concentrated load. Load was applied as a nodal force on the axis of the model. Restraint conditions were imposed at one end of the model so that the deflection of those nodes would

be zero. The difference in results between the two models was computed at the maximum point of deflection.

The analysis was conducted for end mills with lengths of 2.0 to 4.0 inches and diameters of 0.2 to 1.0 inch. Results obtained were non-dimensionalized and are presented in Figure 3.4 below.

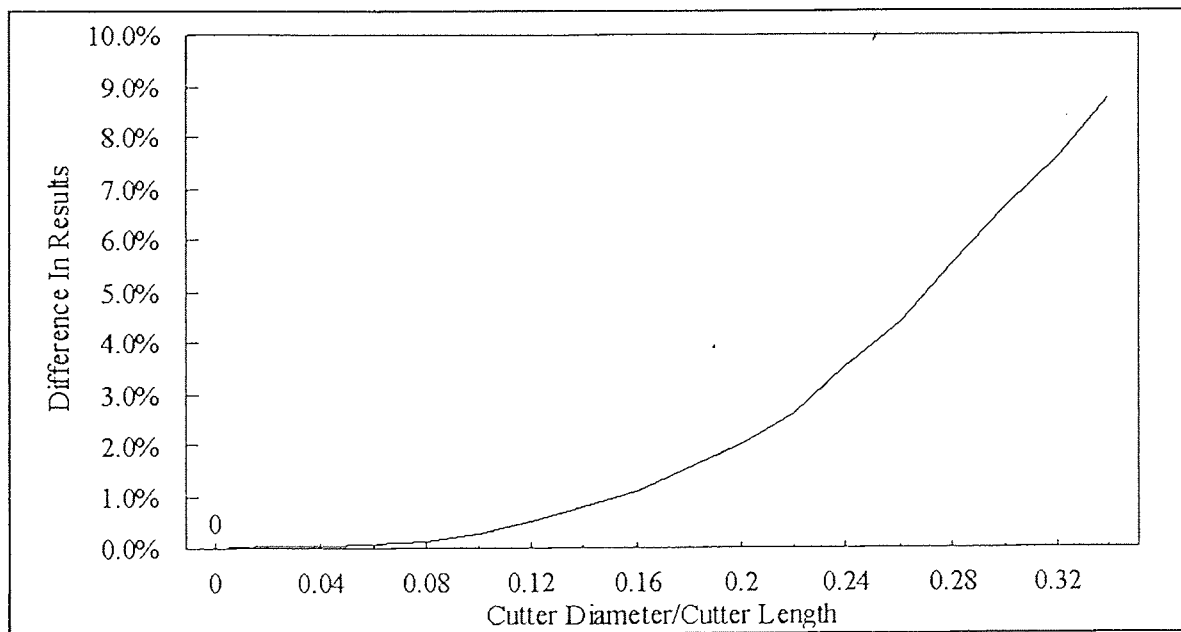


**Figure 3.4** Comparison of flat end mill to ball end mill deflection results under equal loading.

The results demonstrate that when the ratio of cutter diameter to cutter length is small, which is typical for ball end finishing tools, the percentage difference in the deflection results for ball end tools and flat end tools of equal length and diameter is negligible. The assumption of a uniform cross sectional area made in section 3.2.2 will therefore be satisfactory for computing non-linear deflection of ball end mills.

## CHAPTER 4

### EVALUATION OF LINEAR AND NON-LINEAR END MILL DEFLECTION COMPONENTS

#### 4.1 Analysis Methodology

The force and deflection models described in Chapters 2 and 3 were programmed in Fortran on a Sun workstation. Instantaneous force vector data were calculated with the force model. An analysis was then conducted to determine the effects of cutting force variation and cutting depth variation on the linear and non-linear components of end mill deflection. Results were obtained for four flute end mills with diameters of 12.7 mm, 18.14 mm, and 20.0 mm diameters.

Sections 4.2 and 4.3 are concerned strictly with evaluating the separate components of linear and non-linear deflection effecting end mill deformation. Section 4.5 will discuss the transfer of deflection data into a representation of machining error.

#### 4.2 Force Model Output

Inputs to the force model include the experimental constants  $K_t$  and  $K_r$ , the feed per tooth ( $s$ ), cutting depth ( $a_d$ ), cutting width ( $a_r$ ), the diameter of the end mill ( $D$ ), the length of the end mill ( $L$ ), the number of flutes on the end mill ( $N_f$ ), and the end mill helix angle ( $\phi$ ). The model takes this input information and calculates the instantaneous cutting forces

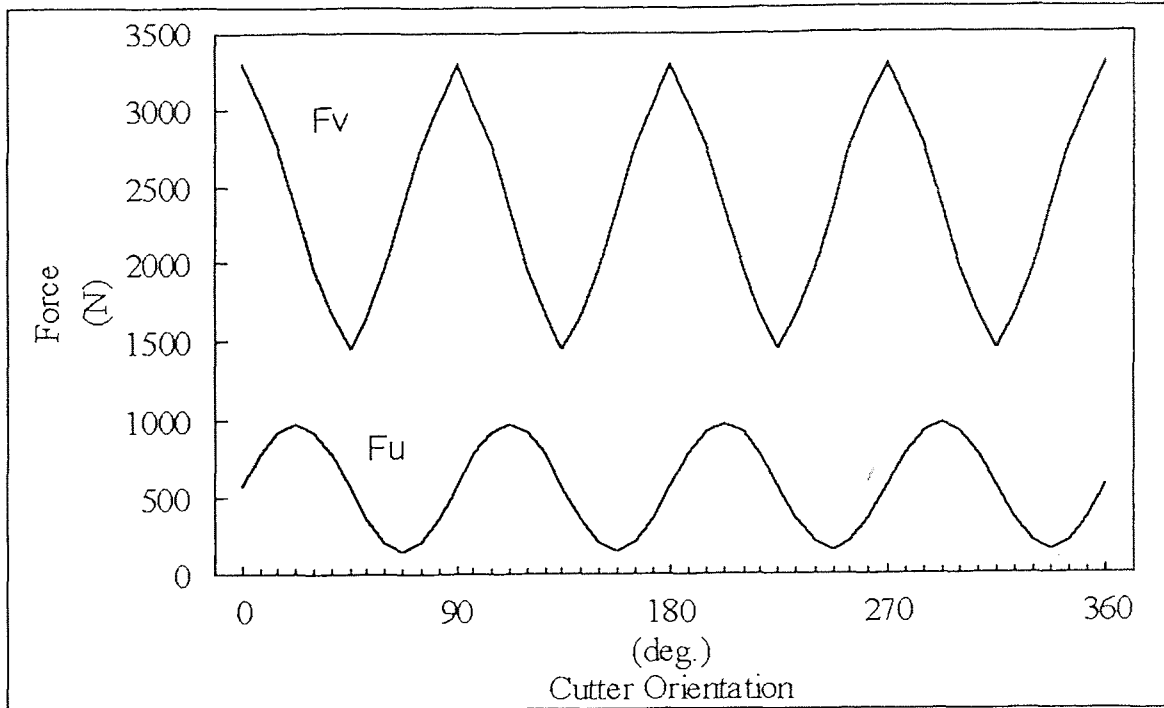


Figure 4.1 Sample force model output.

for the end mill by summing the force vectors acting on the flutes of each divided section in contact with the work piece as described in Chapter 2. In this manner, the force in the cutting direction,  $F_u$ , and the force perpendicular to the cutting direction,  $F_v$ , for the end mills can be calculated. An example output from the force model is depicted in Figure 4.1. The force output depicted above is for a four flute flat end mill with a diameter of 19.05 mm and a 30 degree helix angle. The feed rate in this case was 0.268 mm/revolution,  $s$  was 0.067 mm/tooth,  $a_d$  was 17.4 mm, and  $a_r$  was 9.525 mm. The experimental constants  $K_t$  and  $K_r$  were taken from previous research [Altintas & Spence,91] conducted on a vertical CNC milling machine with a HSS end mill and a 7075-T6 aluminum workpiece. The constants used were  $K_t = 0.317h^{-0.424}$  kN/mm<sup>2</sup> and

$K_r = 0.212h^{-0.217} \text{ kN/mm}^2$  where  $h$  is the average uncut chip thickness .

The cutting force model predicts the cutting forces encountered during one 360 degree revolution of the cutter. As can be seen in Figure 4.1, the force will fluctuate over a range of values. This range varies depending on the cutting conditions. As long as the cutting conditions do not change, the forces over the 360 degree revolution of the cutter will remain the same during the milling process. Each time one of the input cutting conditions changes, however, the force model must be reevaluated. It is interesting to note that although many parameters affect the overall magnitude of the cutting force, the degree of force vector fluctuation experienced is dependent strictly on the selection of the cutting depth [Ber, Rothberg, & Haifa, 1988].

Once the force model has been evaluated, the results can be used to predict the non-linear and linear components of end mill deflection encountered during the milling process. Fluctuations in the instantaneous forces will result in fluctuations in the moments  $M_u$  and  $M_v$ , and a variation in the location at which the point force must be applied to calculate the deflection components. Section 4.3 attempts to show how fluctuations in the cutting force, and resultant point force application will affect the linear and non-linear portions of the end mill deflection.

### 4.3 Evaluation of Deflection Components

#### 4.3.1 Variation with Force

To evaluate the effect of force variation on the linear and non-linear components of end mill deflection, the force model was evaluated for three different values of  $s$  while holding the cutting depth and all other inputs to the program, except  $a_r$ , constant. The value of  $a_r$  was set equal to the radius of the end mill for each case examined. In this manner, it was possible to vary the magnitude of the force and moment while maintaining the same resultant point of force application over the entire 360 degree cutter revolution.

The evaluation was completed for three separate end mills with  $N_f = 4$ ,  $\varphi = 30^\circ$ ,  $L = 40.0$  mm, and diameters of 12.7 mm, 18.14 mm, and 20.0 mm. Cutting depth in each case was set to 19.05 mm. The resultant point of force application was 9.5 mm at a cutter orientation of  $75^\circ$  selected for the evaluation. The feed rate used was 0.268 mm/revolution while  $s$  varied from 0.03 - 0.08 mm/tooth. The experimental constants  $K_t$  and  $K_r$  were the same as those used to compute Figure 4.1.

In order to calculate the linear portion of the deflection using the equations in 3.1, it is necessary to specify the constants  $E_h$  and  $E_r$ . As stated previously,  $E_h$  and  $E_r$  are determined by the structure of the machine, chuck, and collet, and are dependent on the milling machine used. Values of  $E_h$  and  $E_r$  used were based on previous research [Takata & Tsai,89] and correspond to  $0.044 \mu\text{m}/\text{N}$  and  $25.0 \mu\text{m}/\text{Nmm}^2$



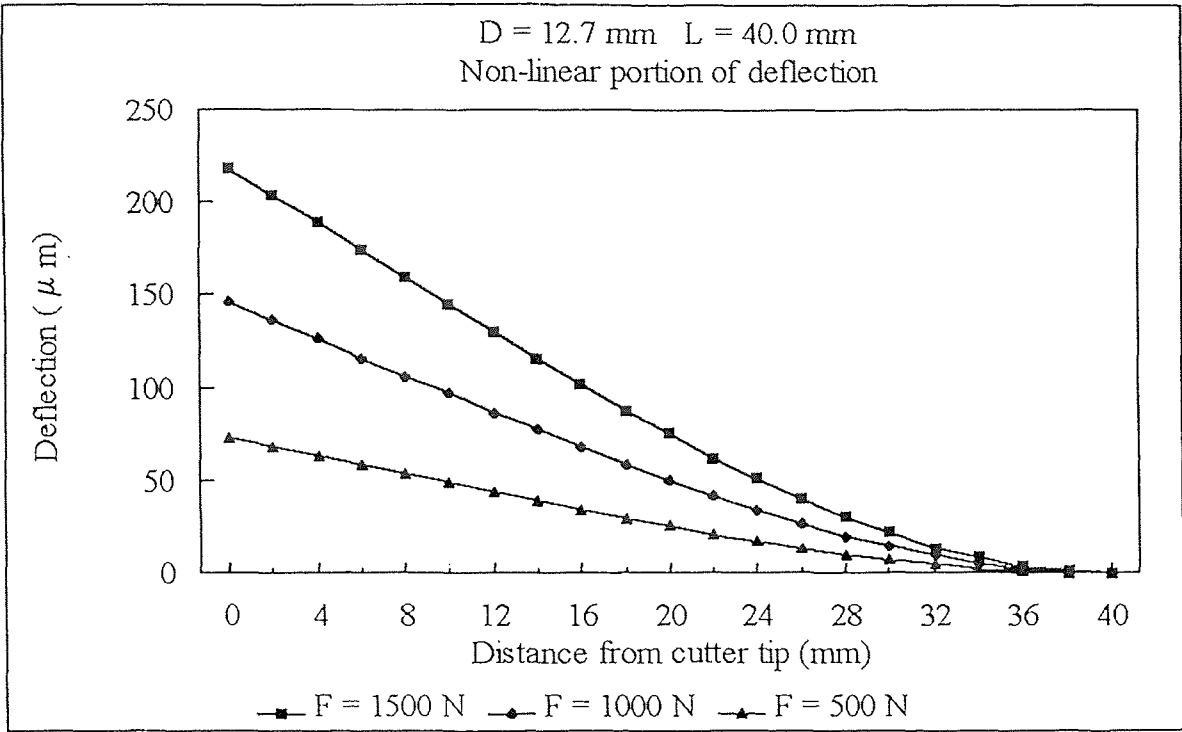


Figure 4.2 Non-linear end mill deflection for various cutting forces D = 12.7 mm.

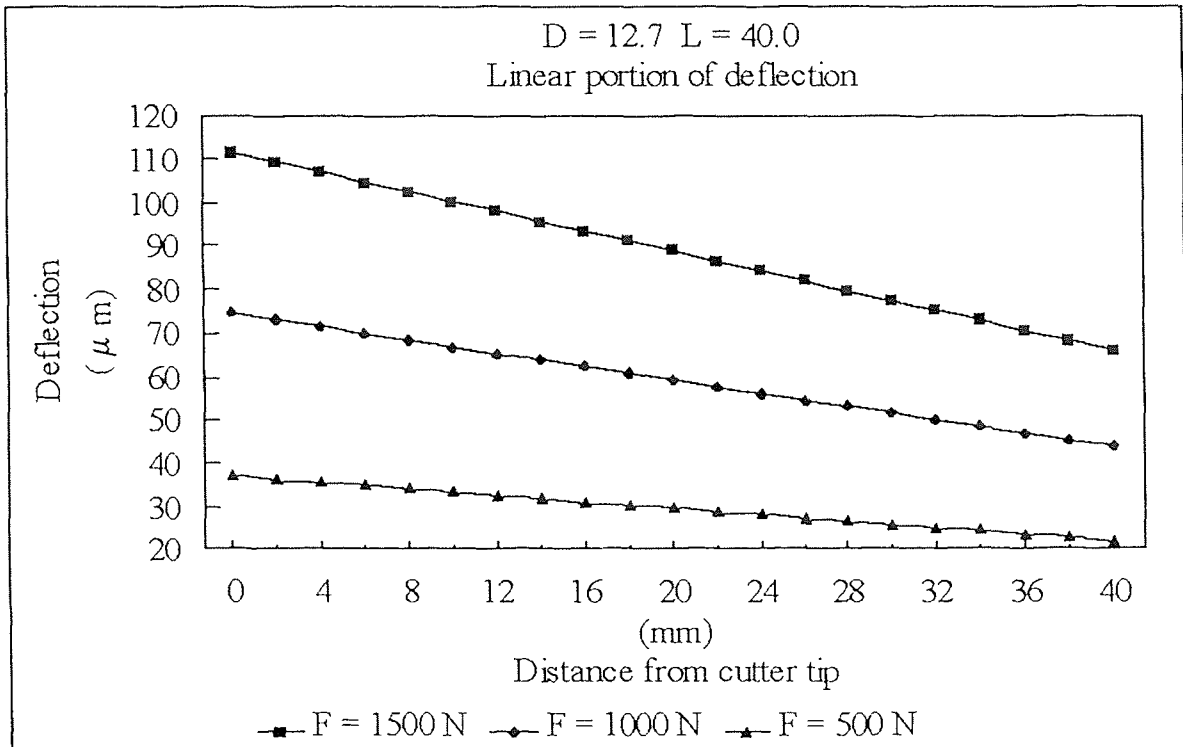
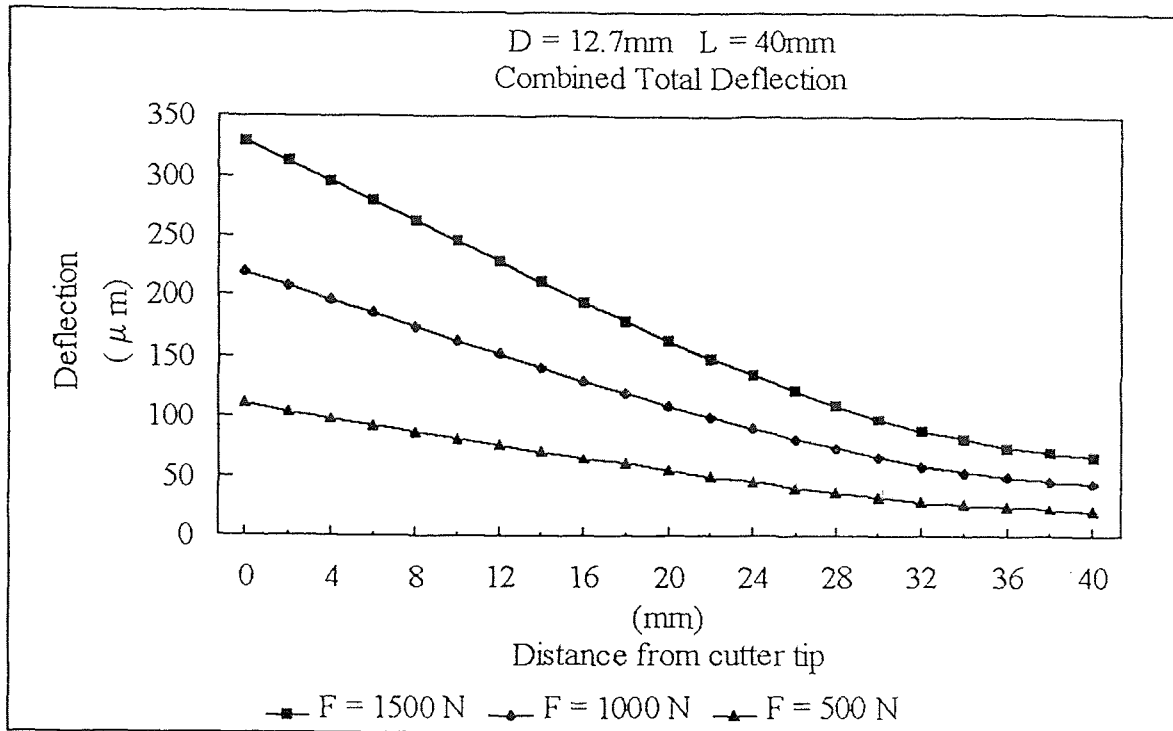


Figure 4.3 Linear end mill deflection for various cutting forces D = 12.7 mm.



**Figure 4.4** Combined end mill deflection for various cutting forces D = 12.7 mm.

respectively for the 12.7 mm end mill,  $0.03 \mu\text{m}/\text{N}$  and  $20.0 \mu\text{m}/\text{Nmm}^2$  for the 18.14 mm end mill, and  $0.01 \mu\text{m}/\text{N}$  and  $15.0 \mu\text{m}/\text{Nmm}^2$  for the 20.0 mm end mill.

Figures 4.2, 4.3, and 4.4 show the results obtained for an end mill with a 12.7 mm diameter and a length of 40.0 mm. A comparison of Figure 4.2 to Figure 4.3 shows that the deflection due to tool deformation is approximately two times the size of the deflection due to the interfaces between the chuck and the collet at the tip of the cutter. At the point corresponding to the top of the cut (19.05 mm), the deflection of the linear and non-linear components are approximately equal. These observations hold true for all magnitudes of the cutting force.

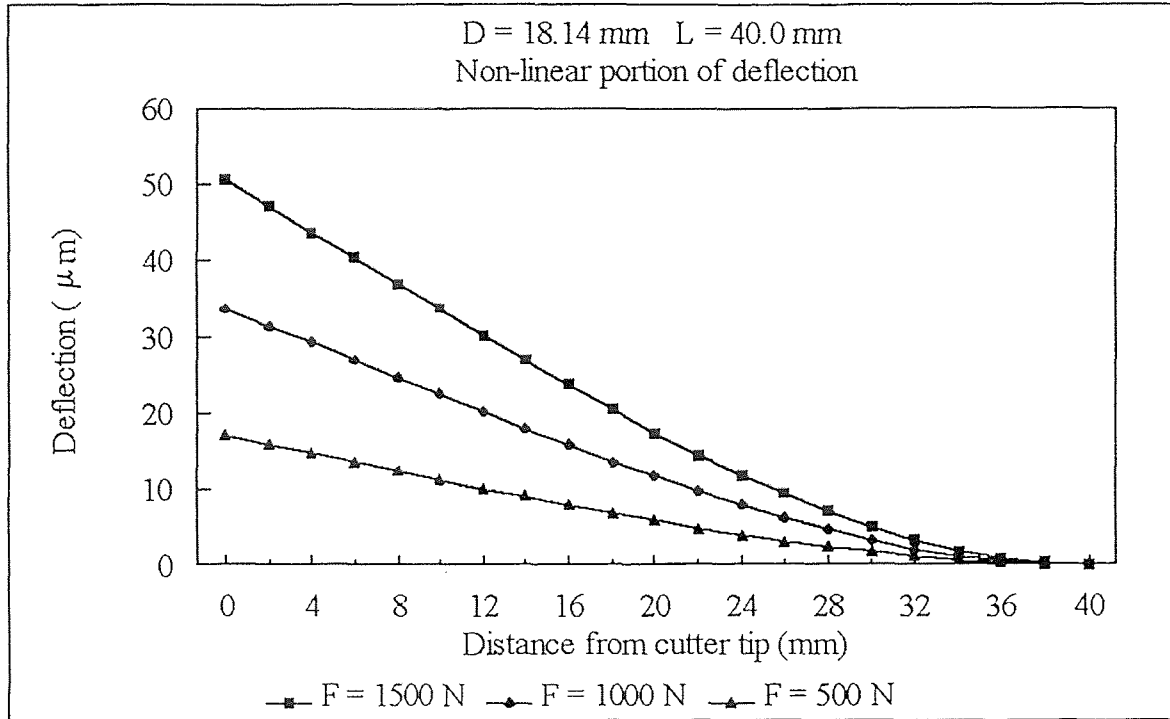


Figure 4.5 Non-linear end mill deflection for various cutting forces D = 18.14 mm.

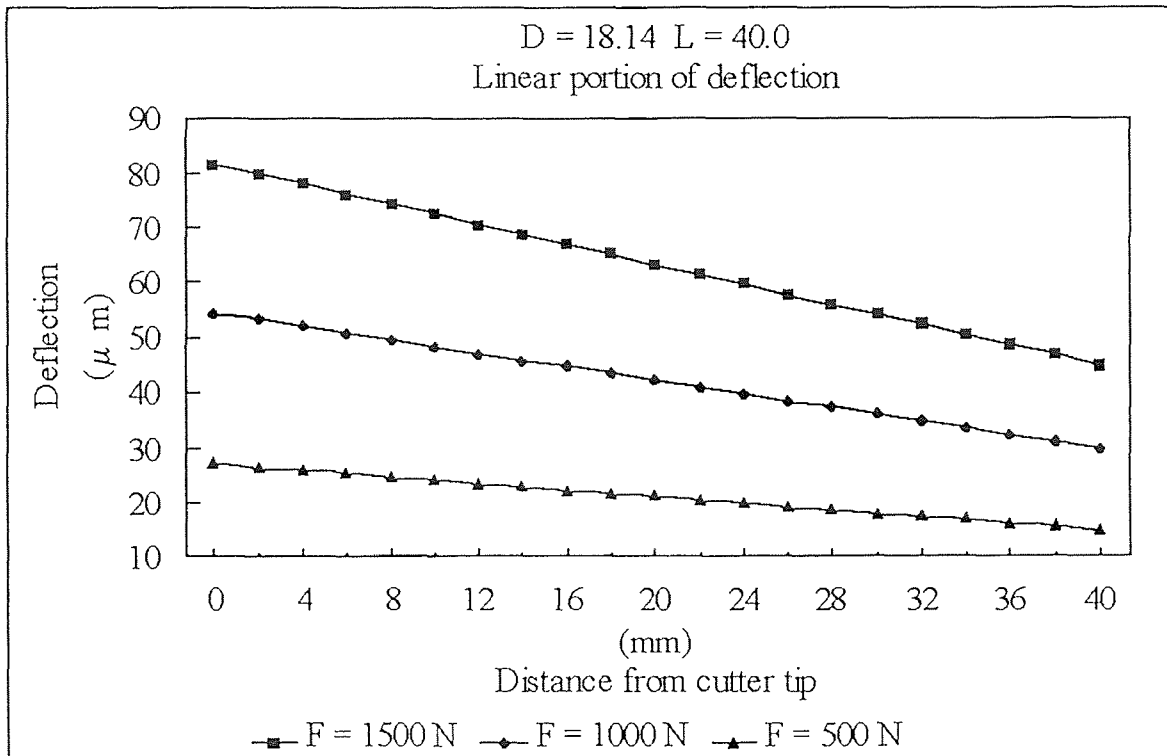
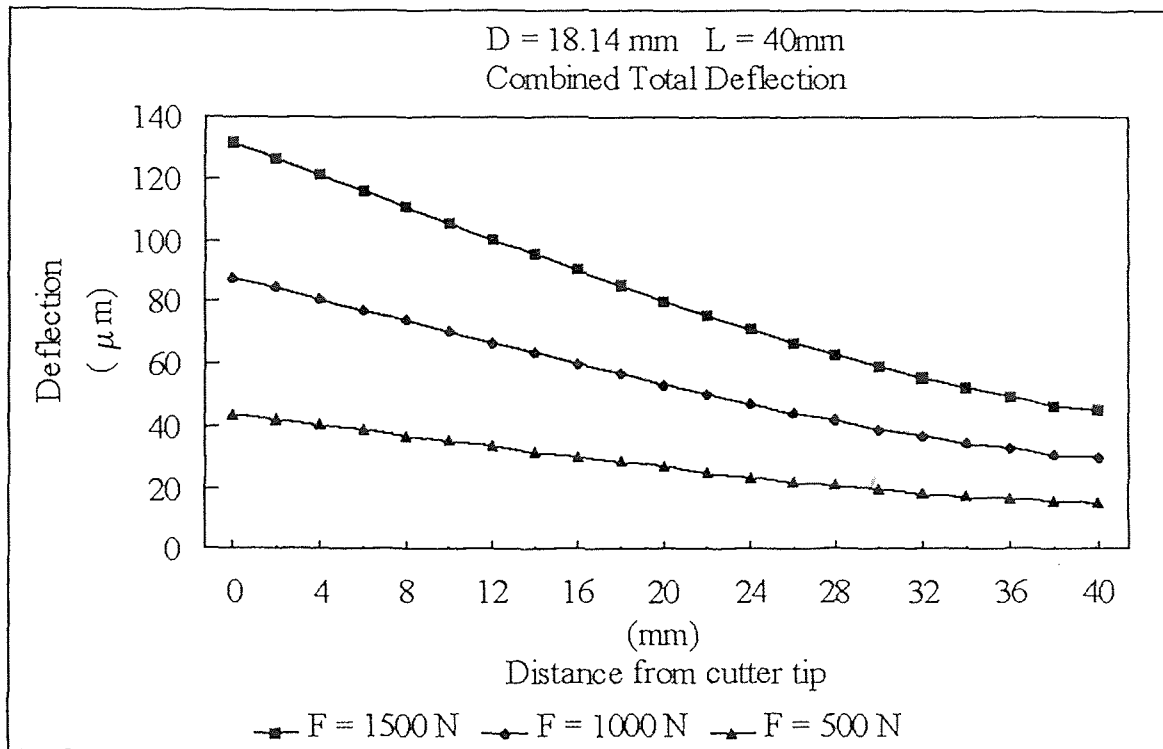


Figure 4.6 Linear end mill deflection for various cutting forces D = 18.14 mm.



**Figure 4.7** Combined end mill deflection for various cutting forces D = 18.14 mm.

Figures 4.5, 4.6, and 4.7 show the results obtained for an end mill with a 18.14 mm diameter and a length of 40.0 mm. Comparing Figure 4.5 to Figure 4.6, we see that the deflection due to tool deformation is less than the deflection due to the interfaces between the tool, the chuck, and the collet. In fact, the horizontal shift of the cutter at the center of the collet ( $\epsilon$  as in Figure 2.3) is almost as large as the maximum non-linear deflection. The non-linear deflection accounts for approximately 39% of the total deflection (Figure 4.7) at the tip of the cutter and, thus, cannot be ignored in an accurate estimation of cutter deflection.

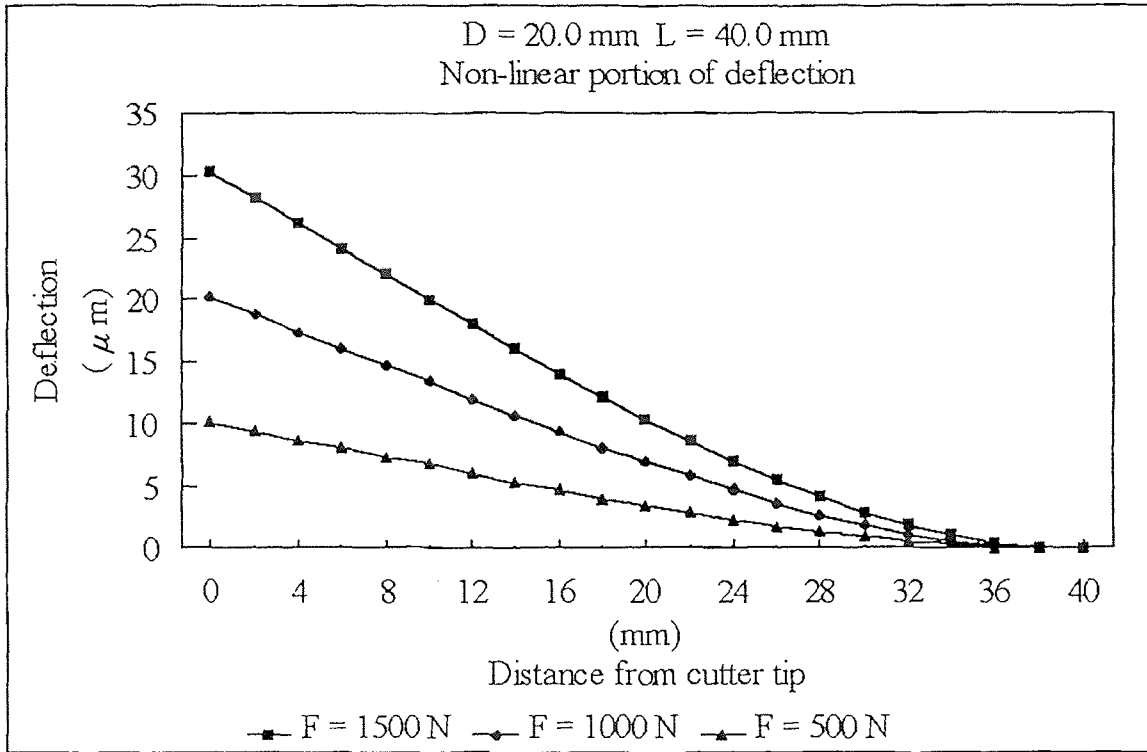


Figure 4.8 Non-linear end mill deflection for various cutting forces D = 20.0 mm.

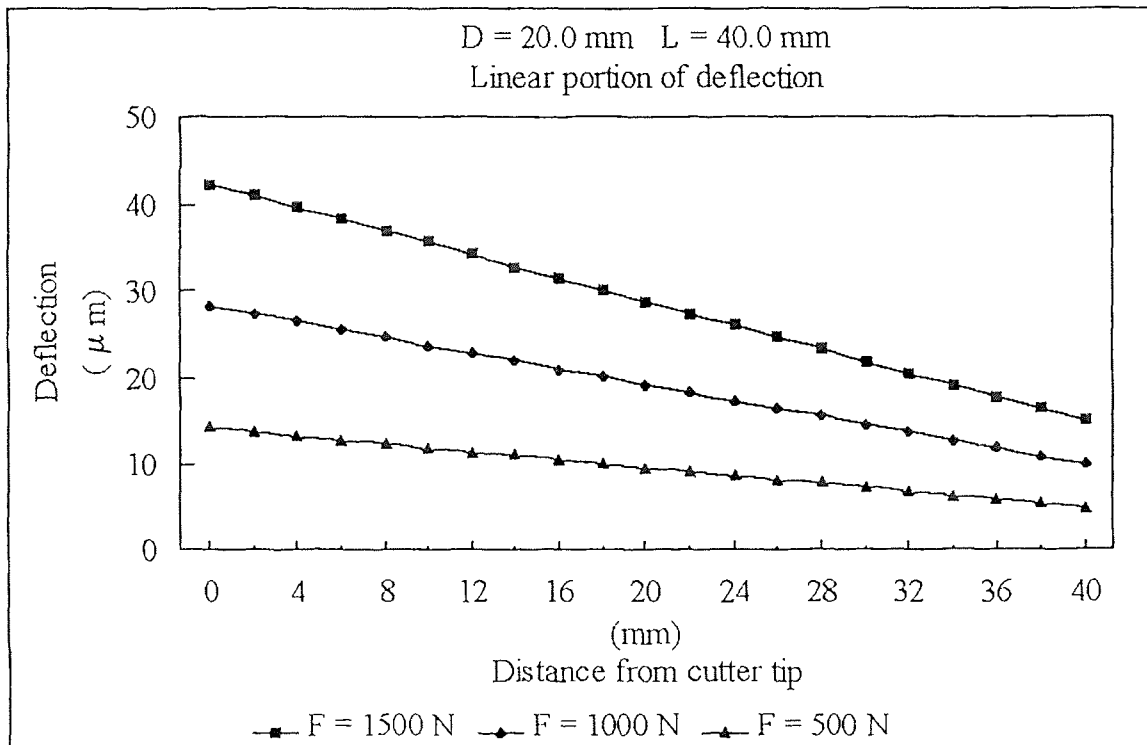
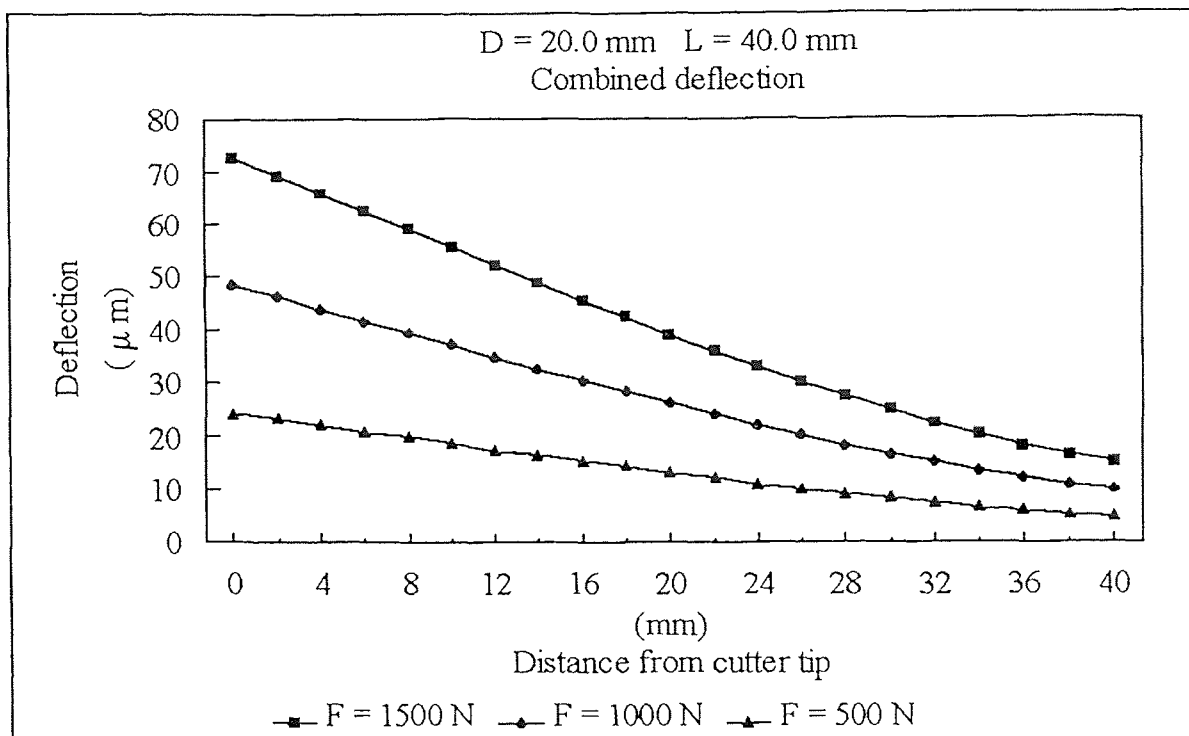


Figure 4.9 Linear end mill deflection for various cutting forces D = 20.0 mm.



**Figure 4.9** Combined end mill deflection for various cutting forces D = 20.0 mm.

Figures 4.7, 4.8, and 4.9 show the results for a 20.0 mm diameter end mill with a length of 40.0 mm. The comparison of linear to non-linear deflection components pictured in Figures 4.7 and 4.8 shows that, as in the case of the 18.14 mm diameter end mill, the deflection due to tool deformation is less than the deflection due to the interfaces between the tool, the chuck, and the collet. The non-linear deflection at the tip of the end mill in this case, however, accounts for just slightly less than half of the total deflection depicted in Figure 4.9. The non-linear deflection of the end mill, thus, still cannot be ignored in the estimation. Figure 4.9 also shows that the overall deflection of the end mill is

quite small. Even at the highest force tested, the total deflection was only 73  $\mu\text{m}$ .

#### 4.3.2 Variation with Cutting Depth

To evaluate the effect of cutting depth variation on the linear and non-linear components of end mill deflection, the force model was evaluated for three separate cutting depths corresponding to 5 mm, 10 mm, and 20 mm, respectively. The value of  $s$  was varied until the average force predicted by the force model for each depth was 750 N. The cutting width in each case study was set equal to the radius of the end mill under examination. All other inputs to the program were initially chosen then held constant. This process was completed, similarly to section 4.3.1, for end mills with the characteristics of  $N_f = 4$ ,  $\varphi = 30^\circ$ ,  $L = 40.0$  mm, and diameters of 12.7 mm, 18.14 mm, and 20 mm. A value of 0.268 mm/revolution was used for the feed rate. The value of  $s$  ranged from 0.0213 - 0.0651 mm/tooth depending on the diameter of the cutter and the cutting depth under examination. The experimental constants  $K_t$  and  $K_r$  used were the same as those used to compute Figure 4.1. The linear deflection constants  $E_h$  and  $E_r$  utilized were the same as those used in section 4.3.1.

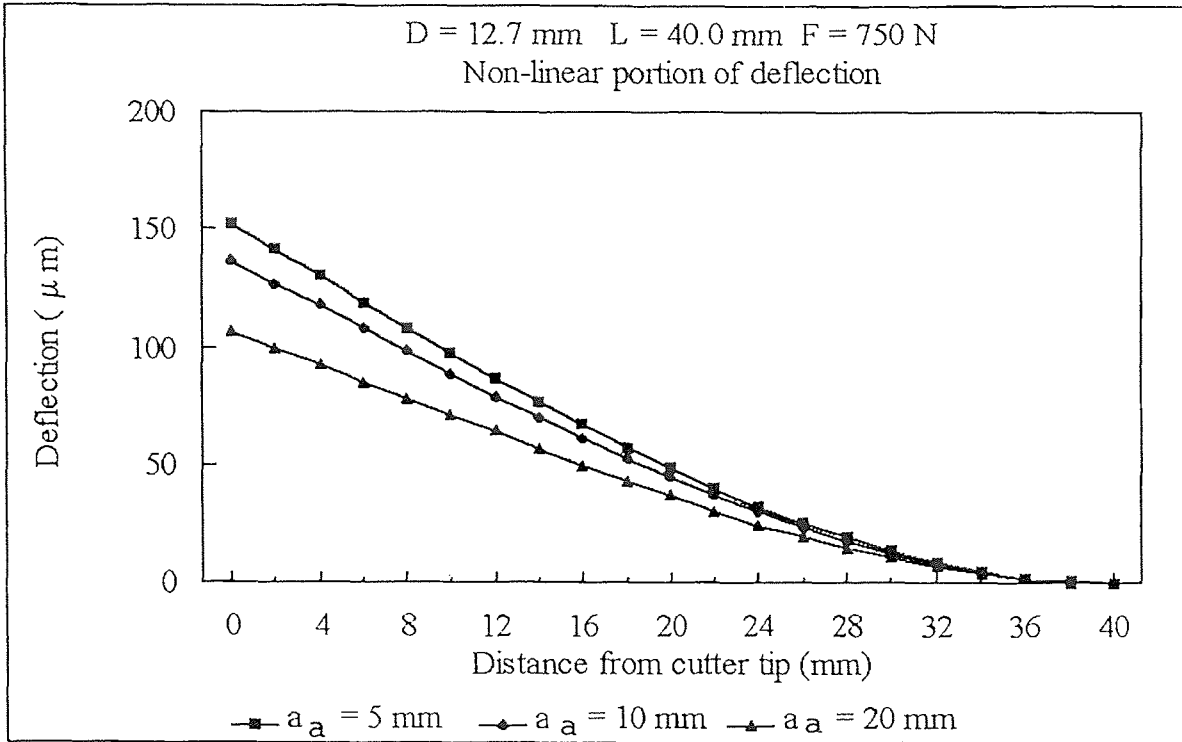


Figure 4.11 Non-linear end mill deflection for various cutting depths with constant force loading, D = 12.7 mm.

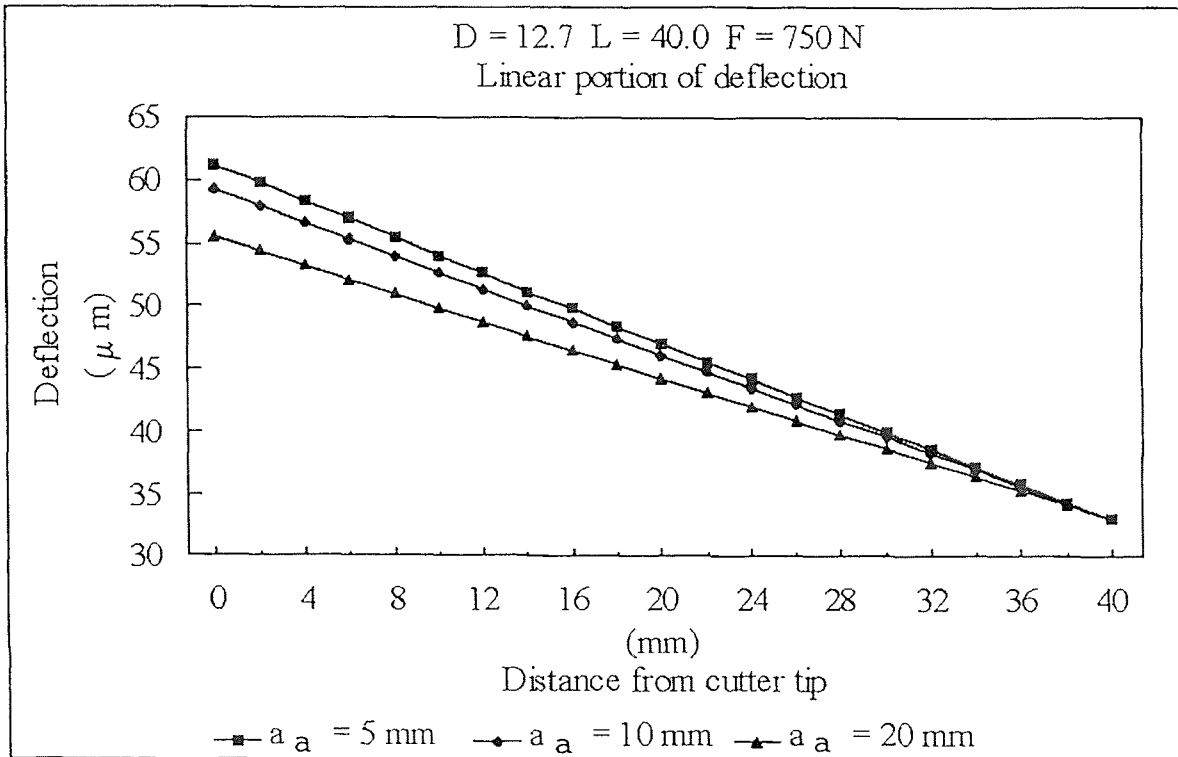
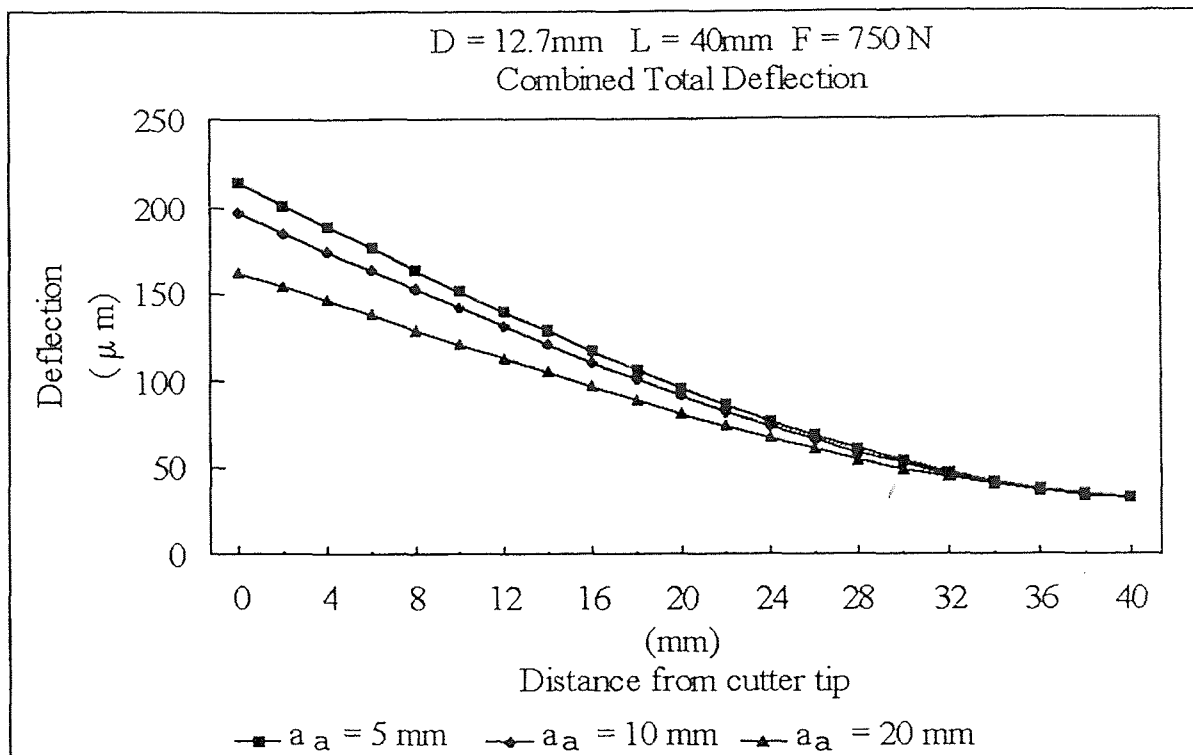


Figure 4.12 Linear end mill deflection for various cutting depths with constant force loading, D = 12.7 mm.





**Figure 4.13** Combined end mill deflection for various cutting depths with constant force loading, D = 12.7 mm.

A comparison of Figures 4.12 and 4.13 shows that the cutting depth has a far greater effect on the non-linear portion of the deflection than on the linear portion of the deflection. Both deflections increase as the depth of cut decreases if the load force is held constant. This is expected due to the fact that the moment arm will be longer for shorter cutting depths.

Figure 4.12 shows that the horizontal displacement in the linear deflection model is not affected by the cutting depth. For the 12.7 mm diameter cutter, comparing Figure 4.11 to Figure 4.12 we see that the non-linear deflection is approximately twice the linear deflection in each case.

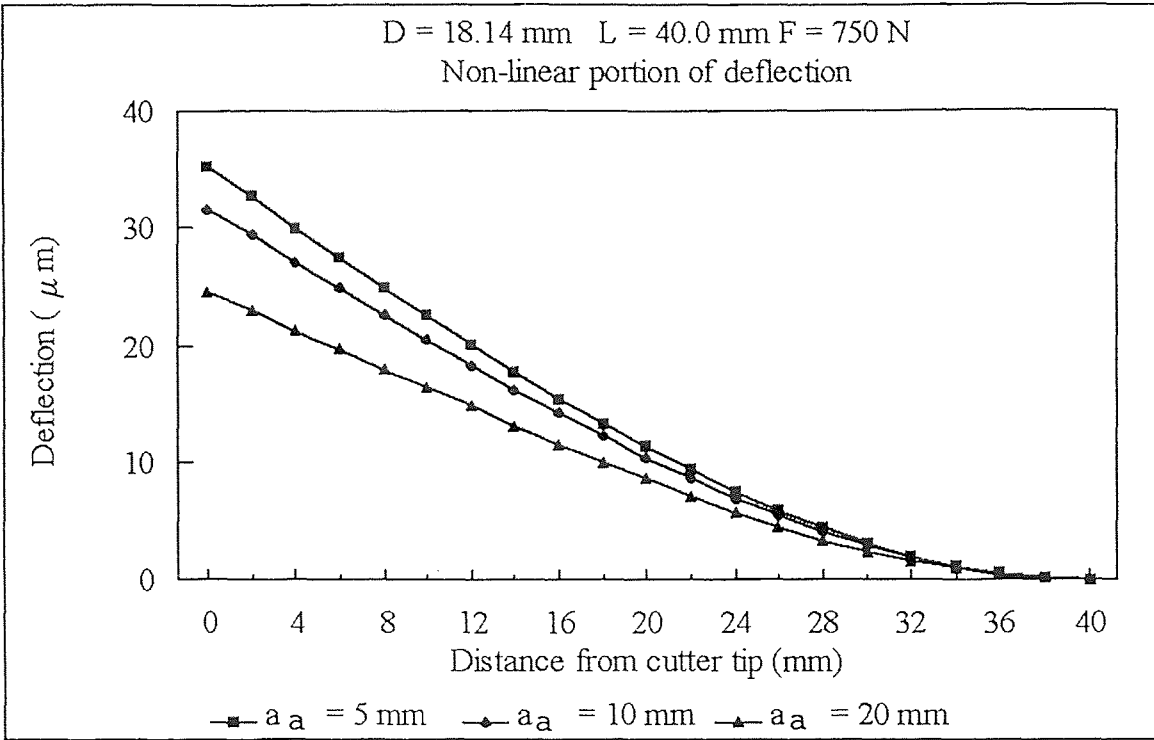


Figure 4.14 Non-Linear end mill deflection for various cutting depths with constant force loading, D = 18.14 mm.

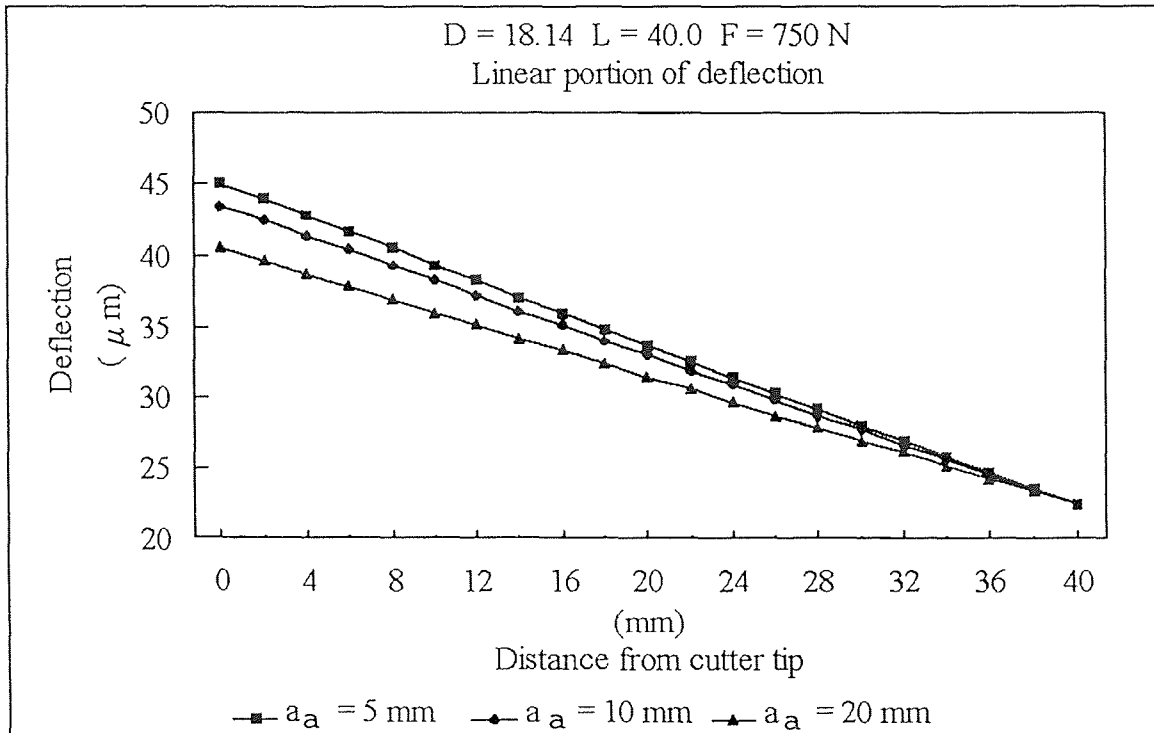
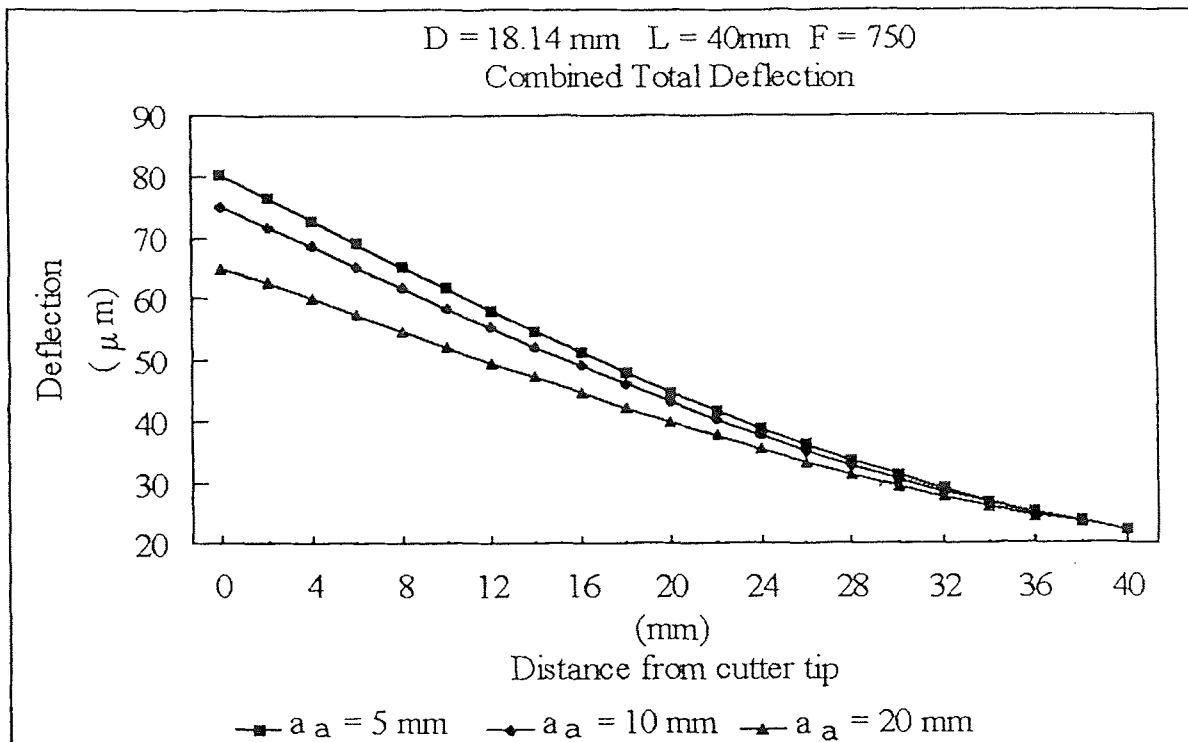


Figure 4.15 Linear end mill deflection for various cutting depths with constant force loading, D = 18.14 mm.



**Figure 4.16** Combined end mill deflection for various cutting depths with constant force loading,  $D = 18.14$  mm.

Examining Figures 4.14, 4.15, and 4.16, it can be seen that the basic observations made for the 12.7 mm diameter end mill hold true for the 18.14 mm diameter end mill. The cutting depth still has a greater effect on the non-linear portion of the deflection than on the linear portion of the deflection. The magnitude of the change however is much smaller. Both deflections still increase as the depth of cut decreases due to an increase in the moment arm.

Comparing Figure 4.14 to Figure 4.15 shows that the non-linear deflection at the shortest cutting depth is 22% smaller than the linear deflection. At the largest cutting depth, the difference is 43%.

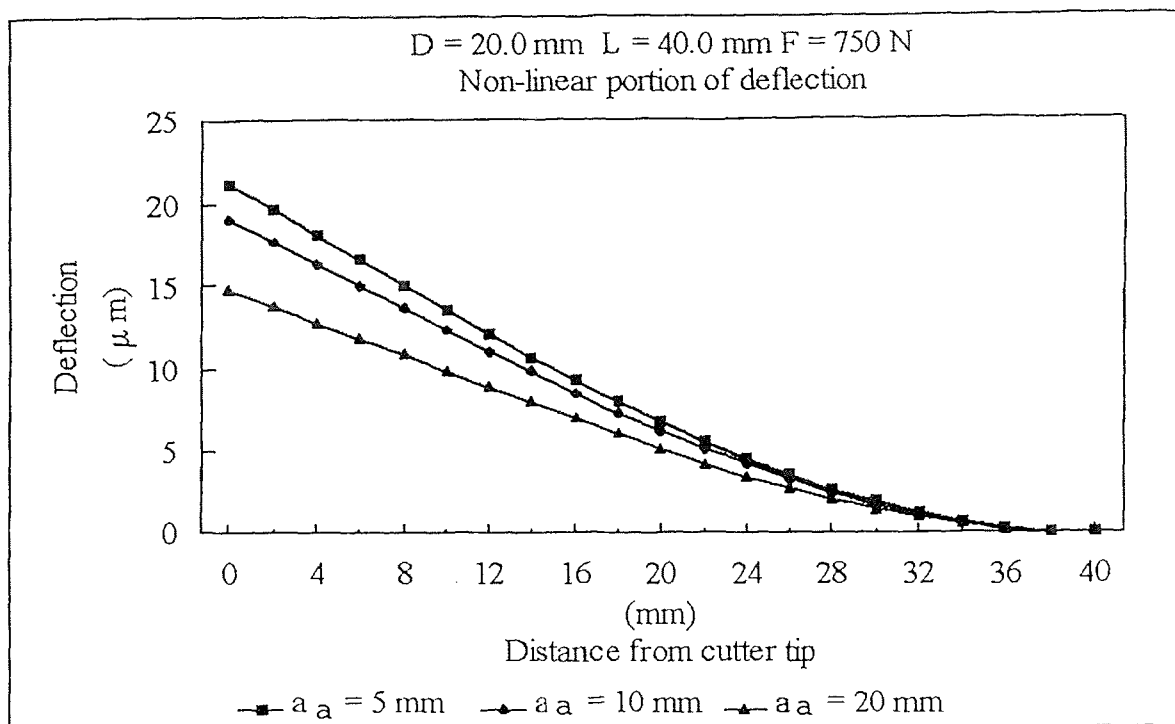


Figure 4.17 Non-linear end mill deflection for various cutting depths with constant force loading, D = 20.0 mm.

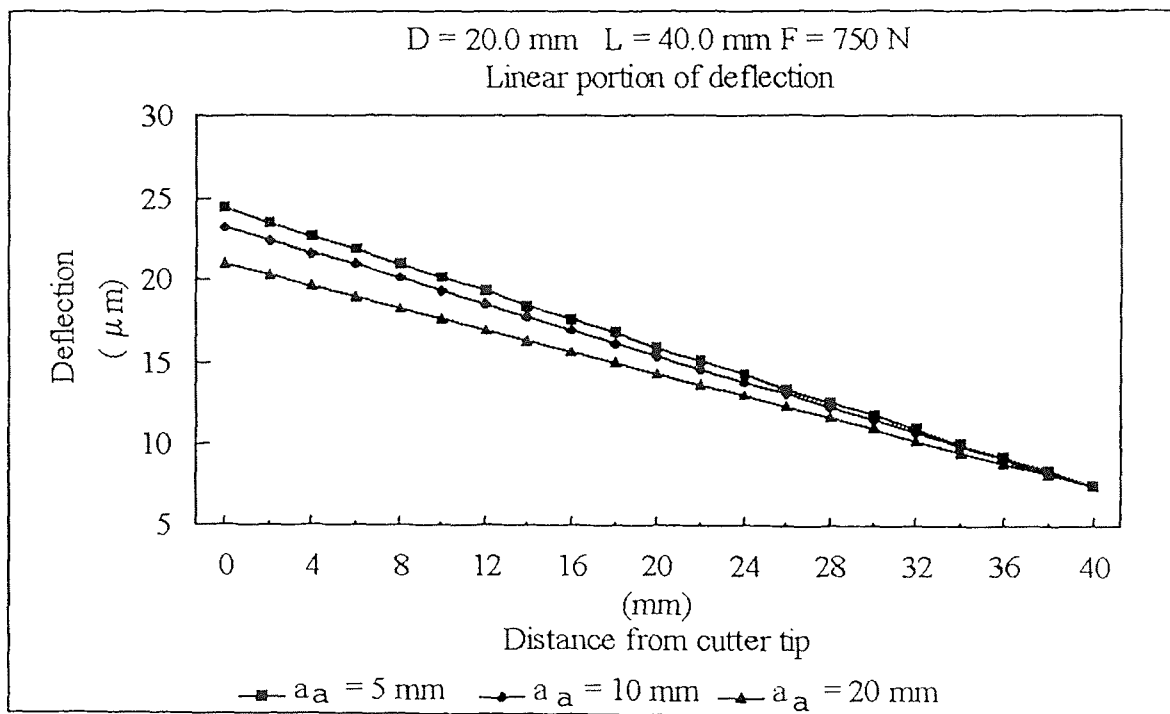
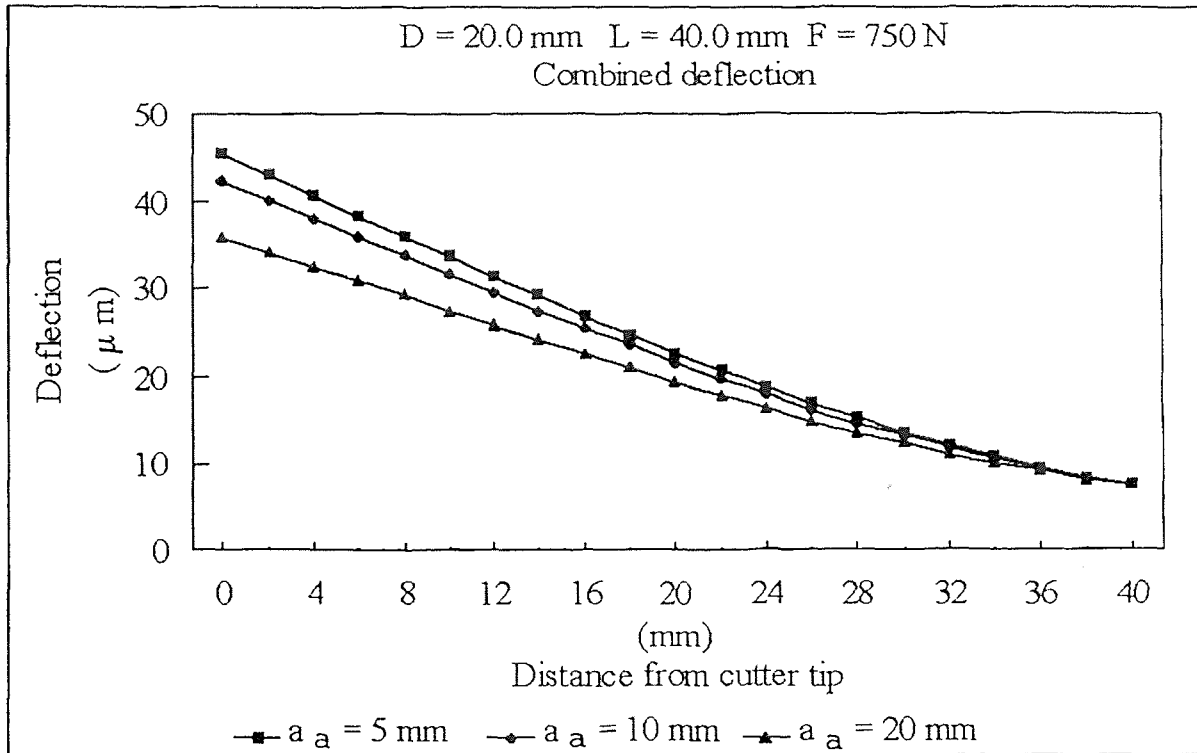


Figure 4.18 Linear end mill deflection for various cutting depths with constant force loading, D = 20.0 mm.



**Figure 4.19** Combined end mill deflection for various cutting depths with constant force loading,  $D = 20.0$  mm.

An examination of Figures 4.17, 4.18, and 4.19, shows that the basic observations stated previously for the 12.7 mm and 18.14 mm diameter end mills still hold true. The cutting depth still has a greater effect on the non-linear portion of the deflection than the linear portion of the deflection. The magnitude of the change is about the same as for the 18.14 mm end mill. The non-linear and linear portions of the deflection in the 20 mm case are approximately of the same magnitude, and the total deflection is very small ( $45 \mu\text{m}$ ) and can probably be ignored in most situations.

#### 4.4 Transferring Deflection Results into a Machining Error Determination

As stated previously in Chapter 2, the machined surface is generated by section  $i,j$  of the flute when that section's angular position,  $\theta_{ij}$ , is coincident with the manner in which the surface is being generated. For surface generation as in Figure 2.1, this would occur when  $\theta_{ij}$  is equal to zero.

As the tool rotates, the position of surface generation,  $S_g$ , moves upward and the machined surface corresponding to point P in Figure 2.1 is generated. Thus, the machining error at each position along the  $w$ -axis, resulting from a deflection of the tool, is estimated from the tool deflection. This would correspond to the deflection in the  $v$  direction for most types of milling cuts. This says that to generate a prediction of the surface error along the depth of the cut for a given set of milling conditions, when  $\theta_{ij}$  is equal to zero, the total deflection of the end mill at the point  $W_i$  along the cutter,  $\delta(W_i)$ , axis must be calculated. This deflection is equal to the surface error at height  $W_i$  from the bottom of the cut.

## CHAPTER 5

### CONCLUSION

#### 5.1 Conclusions

This study has shown that both linear deflection due to the interfaces between an end milling tool, chuck and collet, and non-linear deflection due to actual tool bending have significant effects on the total deflection experienced during end milling. This has been demonstrated for a range of cutting forces and cutting depths. At no point in the study did either of the modes of deflection prove to be insignificant.

Variations in cutting depth have been shown to effect non-linear deflection more than linear deflection. Variations in cutting force tend to effect both deflections equally. During the problem formulation, the deflection model used in this study was demonstrated to be effective for ball end mills as well as flat end mills.

#### 5.2 Suggestions for Future Work

During the formulation part of this work, a model was formulated for the prediction of cutting forces encountered during milling for ball end mills. This model was not used in the analysis because there was no way to validate it. One suggestion for future work is to run some cutting experiments to validate this force model.

## REFERENCES

- [Altintas & Spence,91] Altintas, Y., A. Spence, "End Milling Force Algorithms for CAD Systems," Annals of the CIRP Vol. 40/1, 1991, pp. 31-34.
- [Armarego, E.J.A.,82] Armarego, E.J.A., UNESCO-CIRP seminar on Manufacturing Technology, Singapore, 1982.
- [Ber, Rothberg, & Haifa,88] Ber, A., J. Rothberg, S. Zombach, "A Method for Cutting Force Evaluation of End Mills," Annals of the CIRP Vol. 37/1, 1988, pp. 37-40.
- [Bertok,83] Bertok, P., "A System for Monitoring the Machining Operation by Referring to a Predicted Cutting Torque Pattern," Annals of CIRP Vol. 32/1, 1983, pp. 439-444.
- [Kline,82] Kline, W.A., "The Prediction of Cutting Forces in End Milling with Application to Cornering Cuts," MTDR Vol. 22, 1982, pp. 7-22.
- [Kline, DeVor, & Shareef,82] Kline, W.A., R.E. DeVor, I.A. Shareef, "The Prediction of Surface Accuracy in End Milling," Journal of Engineering for Industry Vol.104, pp. 272-278.
- [Kops & Vo,90] Kops, L., D.T. Vo, "Determination of the Equivalent Diameter of an End Mill Based on its Compliance," Annals of CIRP Vol. 39/1, 1990, pp. 93-96.
- [Takata & Tsai,89] Takata, S., M.D. Tsai, and M. Inui, "A Cutting Simulation System for Machinability Evaluation Using a Workpiece Model," Annals of CIRP Vol. 38/1, 1989, pp. 417-420.
- [Tsai & Takata,90] Tsai, M.D., S. Takata, M. Inui, F. Kimura, T. Sata, "Prediction of Chatter Vibration by Means of a Model-Based Cutting Simulation System," Annals of CIRP Vol. 39/1, 1990, pp. 447-450.
- [Wang,87] Wang, K.K., "Application of Solid Modeling to Automate Machining Parameters for Complex Parts," Proceedings of CIRP Manufacturing Seminar, Pen State University, 1987, pp. 33-37.
- [Whitfield, R.C. & Armarego, E.J.A.,88] Whitfield, R.C., E.J.A. Armarego, *Presentation Charts and Notes from the Fourth International Conference on Manufacturing Engineering*, Institute of Engineering Australia, Brisbane, 1988, pp. 206-211.



REFERENCES  
(Continued)

[Whitfield, R.C.,88] Whitfield, R.C., *Cutting Models for Computerized End-Milling Force Predictions*, Ph.D. Thesis, University of Melbourne, 1988.